UNIVERSITY OF HELSINKI
DEPARTMENT OF PHYSICS

UNIVERSITY OF HELSINKI

REPORT SERIES IN GEOPHYSICS

No 66

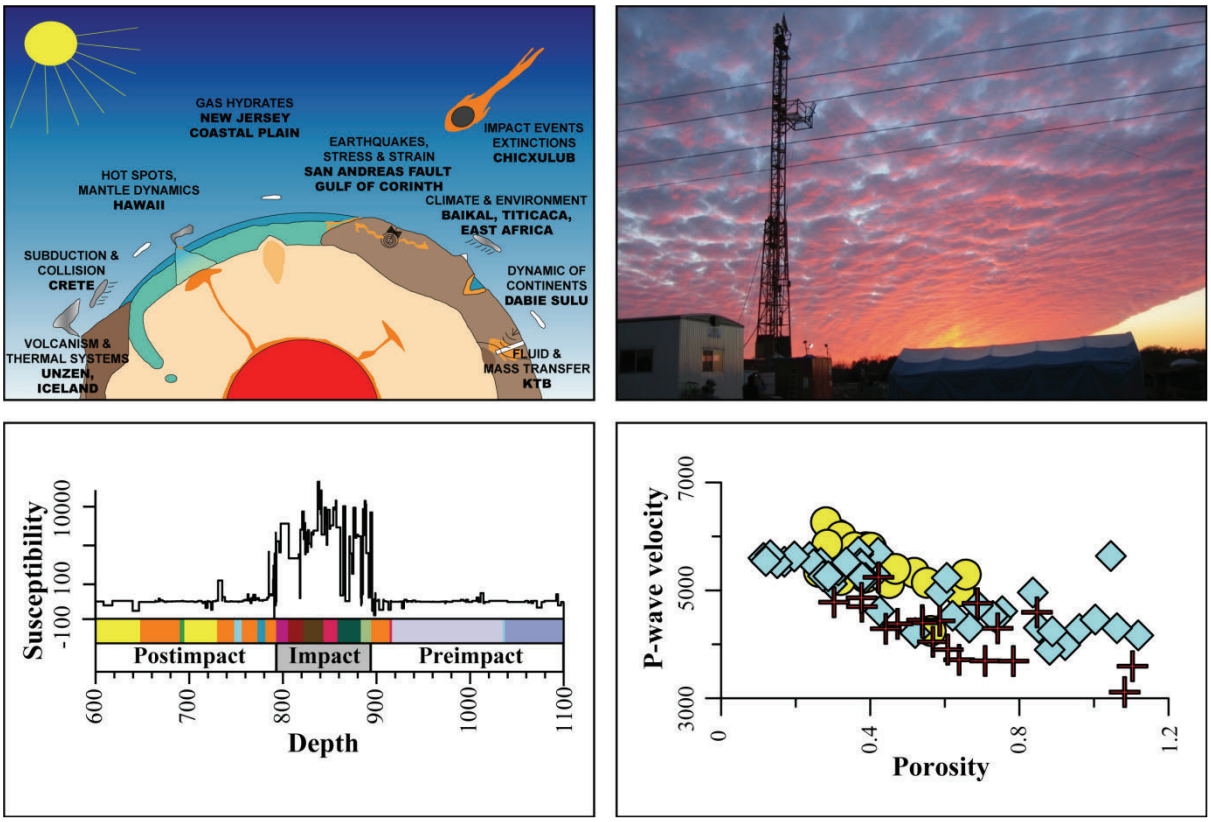

PHYSICAL PROPERTIES OF DEEP DRILL CORES – IMPLICATIONS FOR METEORITE IMPACT EFFECTS AND CRUSTAL STRUCTURES

Tiiu Elbra

HELSINKI 2011

UNIVERSITY OF HELSINKI
DEPARTMENT OF PHYSICS

REPORT SERIES IN GEOPHYSICS
No 66

PHYSICAL PROPERTIES OF DEEP DRILL CORES – IMPLICATIONS FOR METEORITE IMPACT EFFECTS AND CRUSTAL STRUCTURES

Cover picture:
Top left: Illustration of the International Continental Scientific Drilling Program activities
Top right: Eyreville drilling site, Chesapeake Bay impact structure, U.S.A.
Bottom left: Magnetic susceptibility of impact, post- and pre-impact rocks, Chicxulub impact structure, Mexico
Bottom right: Correlation between porosity and p-wave velocity of various lithologies, Outokumpu, Finland

Tiiu Elbra

HELSINKI 2011

Supervisor:

Prof. Lauri J. Pesonen
Division of Geophysics and Astronomy
Department of Physics
University of Helsinki
Helsinki, Finland

Pre-examiners:

Res. prof. Ilmo Kukkonen
Geological Survey of Finland
Espoo, Finland

Dr. Jüri Plado
Department of Geology
Institute of Ecology and Earth Sciences
Tartu, Estonia

Opponent:

Res. prof. Gunther Kletetschka
Department of Physics
Catholic University of America
Washington DC, USA

Custos:

Prof. Lauri J. Pesonen
Division of Geophysics and Astronomy
Department of Physics
University of Helsinki
Helsinki, Finland

Report Series in Geophysics No. 66
ISBN 978-952-10-6875-1 (paperback)
ISSN 0355-8630
Helsinki 2011
Unigrafia

ISBN 978-952-10-6876-8 (pdf)
http://ethesis.helsinki.fi
Helsinki 2011
Helsingin yliopiston verkkojulkaisut

PHYSICAL PROPERTIES OF DEEP DRILL CORES – IMPLICATIONS FOR METEORITE IMPACT EFFECTS AND CRUSTAL STRUCTURES

Tiiu Elbra

ACADEMIC DISSERTATION IN GEOPHYSICS

To be presented, with the permission of the Faculty of Science of the University of Helsinki for public criticism in the Auditorium B123 of Exactum, Gustaf Hällströminkatu 2b, on May 13th, 2011, at 12 o'clock noon.

Helsinki 2011

Table of Contents

Abstract

Physical properties provide valuable information about the nature and behavior of rocks and minerals. The changes in rock physical properties generate petrophysical contrasts between various lithologies, for example, between shocked and unshocked rocks in meteorite impact structures or between various lithologies in the crust. These contrasts may cause distinct geophysical anomalies, which are often diagnostic to their primary cause (impact, tectonism, etc). This information is vital to understand the fundamental Earth processes, such as impact cratering and associated crustal deformations. However, most of the present day knowledge of changes in rock physical properties is limited due to a lack of petrophysical data of subsurface samples, especially for meteorite impact structures, since they are often buried under post-impact lithologies or eroded. In order to explore the uppermost crust, deep drillings are required.

This dissertation is based on the deep drill core data from three impact structures: (i) the Bosumtwi impact structure (diameter 10.5 km, 1.07 Ma age; Ghana), (ii) the Chesapeake Bay impact structure (85 km, 35 Ma; Virginia, U.S.A.), and (iii) the Chicxulub impact structure (180 km, 65 Ma; Mexico). These drill cores have yielded all basic lithologies associated with impact craters such as post-impact lithologies, impact rocks including suevites and breccias, as well as fractured and unfractured target rocks. The fourth study case of this dissertation deals with the data of the Paleoproterozoic Outokumpu area (Finland), as a non-impact crustal case, where a deep drilling through an economically important ophiolite complex was carried out.

The focus in all four cases was to combine results of basic petrophysical studies of relevant rocks of these crustal structures in order to identify and characterize various lithologies by their physical properties and, in this way, to provide new input data for geophysical modellings. Furthermore, the rock magnetic and paleomagnetic properties of three impact structures, combined with basic petrophysics, were used to acquire insight into the impact generated changes in rocks and their magnetic minerals, in order to better understand the influence of impact.

The obtained petrophysical data outline the various lithologies and divide rocks into four domains. Based on target lithology the physical properties of the unshocked target rocks are controlled by mineral composition or fabric, particularly porosity in sedimentary rocks, while

sediments result from diverse sedimentation and diagenesis processes. The impact rocks, such as breccias and suevites, strongly reflect the impact formation mechanism and are distinguishable from the other lithologies by their density, porosity and magnetic properties.

The numerous shock features resulting from melting, brecciation and fracturing of the target rocks, can be seen in the changes of physical properties. These features include an increase in porosity and subsequent decrease in density in impact derived units, either an increase or a decrease in magnetic properties (depending on a specific case), as well as large heterogeneity in physical properties. In few cases a slight gradual downward decrease in porosity, as a shock-induced fracturing, was observed. Coupled with rock magnetic studies, the impact generated changes in magnetic fraction – the shock-induced magnetic grain size reduction, hydrothermal- or melting-related magnetic mineral alteration, shock demagnetization and shock- or temperature-related remagnetization – can be seen.

The Outokumpu drill core shows varying velocities throughout the drill core depending on the microcracking and sample conditions. This is similar to observations by Kern et al., (2009), who also reported the velocity dependence on anisotropy. The physical properties are also used to explain the distinct crustal reflectors as observed in seismic reflection studies in the Outokumpu area. According to the seismic velocity data, the interfaces between the diopside-tremolite skarn layer and either serpentinite, mica schist or black schist are causing the strong seismic reflectivities.

Acknowledgements

I give my sincere thanks to all the people who helped me during the course of my doctoral studies at the University of Helsinki.

I would like to express my foremost gratitude to my supervisor Prof. Lauri J. Pesonen for giving me the opportunity to work in the International Continental Scientific Drilling Program (ICDP) and Outokumpu drilling projects. His constructive advice throughout my studies was invaluable.

I thank the pre-examiners of this thesis, Dr. Jüri Plado (University of Tartu, Estonia) and Res. Prof. Ilmo Kukkonen (Geological Survey of Finland), for their constructive reviews, which helped to improve the thesis significantly.

I am grateful to my current and previous colleagues and friends from the Department of Physics, University of Helsinki, especially Dr. Tomáš Kohout, MSc. Robert Klein, MSc. Selen Raiskila, Dr. Johanna Salminen, MSc. Michał Bucko and Dr. Fabio Donadini for their support and advice.

I am indebted to my co-authors Prof. Edward Hæggström, MSc. Ronnie Karlqvist, Dr. Agnes Kontny, Phil.Lic. Ilkka Lassila, Dr. Norbert Schleifer, and MSc. Christina Schell for their help.

My sincere thanks to Dr. Meri-Liisa Airo, Dr. Lucy E. Edwards, Dr. Gregory S. Gohn, Dr. Thomas Kenkmann, Prof. Christian Koeberl, Prof. Martti Lehtinen, Dr. Sibylle Mayr, Dr. Satu Mertanen, Dr. Yuri Popov, Dr. Petr Pruner, Prof. Wolf Uwe Reimold, and Prof. Jaime Urrutia-Fucugauchi for their co-operation. Thanks also to the summer-students Mr. Aurélien Cheron, Ms. Ulpu Leijala and MSc. Mariliis Rõõmussaar for assistance in the laboratory.

The financial support for conducting this PhD-project as well as presenting the results at conferences was provided by Vilho, Yrjö and Kalle Väisälä Foundation, K.H. Renlund Foundation, Outokumpu Foundation, CIMO, Ella and Georg Ehrnrooth Foundation, Magnus Ehrnrooth Foundation, Emil Aaltonen Foundation, Oskar Öflund Foundation, Academy of Finland bilateral research exchange, and University of Helsinki Chancellor's travel grant.

Finally, my sincerest thanks go to my family, relatives and friends, especially my parents Ludmilla and Toivo Elbra and my sister Elen Elbra, for their patience and continuous support.

This thesis is based on the following five papers, which are referred to in the text by their Roman numerals:

I Elbra, T., Kontny, A., Pesonen, L.J., Schleifer, N., Schell C., 2007. Petrophysical and paleomagnetic data of drill cores from the Bosumtwi impact structure, Ghana. *Meteoritics & Planetary Science*, 42, Nr 4/5, 829–838.

II Kontny, A., Elbra, T., Just, J., Pesonen, L.J., Schleicher, A., Zolk, J., 2007. Petrography and shock-related remagnetization of pyrrhotite in drill cores from the Bosumtwi Impact Crater Drilling Project, Ghana. *Meteoritics & Planetary Science*, 42, Nr 4/5, 811–827.

III Elbra, T., Kontny, A., Pesonen, L.J., 2009. Rock-magnetic properties of the ICDP-USGS Eyreville core, Chesapeake Bay impact structure, Virginia, USA. In Gohn, G.S., Koeberl, C., Miller, K.G., and Reimold, W.U., eds., Deep drilling in the Chesapeake Bay impact structure: *Geological Society of America Special Papers* 2009, 458, p. 119-135.

IV Elbra, T., Pesonen, L.J. Physical properties of Yaxcopoil-1 deep drill core, Chicxulub impact structure, Mexico. *Meteoritics & Planetary Science* (revised).

V Elbra, T., Karlqvist, R., Lassila, I., Hæggström, E., Pesonen, L.J., 2011. Laboratory measurements of the seismic velocities and other petrophysical properties of the Outokumpu Deep Drill Core samples, Finland. *Geophysical Journal International*, 184, 405–415.

Authors' contribution to the publications

Paper **I**: Tiiu Elbra was the leading author. She conducted all the petrophysical and paleomagnetic measurements at the University of Helsinki and combined these with the experimental data acquired in Heidelberg and Leoben. She was responsible for data analysis and interpretation, writing most of the manuscript, and handling the review and proof stage.

Paper **II**: Tiiu Elbra conducted the rock magnetic measurements and analysis, including magnetic hysteresis and temperature dependence of magnetic susceptibility, at the University of Helsinki. These results were then combined with data acquired in University of Heidelberg. Tiiu also contributed to writing the manuscript.

Paper **III**: Tiiu Elbra was the leading author. She conducted all the petrophysical, rock magnetic and paleomagnetic measurements at University of Helsinki and combined these with the experimental data obtained in Karlsruhe. She conducted magnetic susceptibility measurements of the full core at the US Geological Survey. She was responsible for data analysis and interpretation, and did most of the manuscript writing, except for the section about implications for magnetic modeling. She was responsible for handling the manuscript during the review and proof stage.

Paper **IV**: Tiiu Elbra was the leading author. She conducted all the petrophysical, rock magnetic and paleomagnetic measurements, and was responsible for data analysis, interpretation, manuscript writing and handling.

Paper **V**: Tiiu Elbra was the leading author. She conducted all the petrophysical, including P-wave velocity, measurements at laboratory pressure conditions and was actively participating in ultrasonic seismic velocity experiments at *in situ*-like pressure conditions. She was responsible for data analysis and interpretation, and did most of the manuscript writing, except for the section about ultrasonic instrument description. She also handled the manuscript during the review and proof stage.

1 Introduction

Physical properties are essential in understanding the nature and behavior of materials, and are necessary in various disciplines – geology, geophysics, material science, environmental studies and geotechnical engineering. They are an important aspect in detecting the natural resources, such as oil, gas and ores, and in reconstructions of the mineral deposits. Furthermore, physical properties provide insight into nature of the crustal structures as well as into fundamental Earth processes, such as impact cratering, the origin and source of the Earth's magnetic field, and in tracing its history through geologic time (*Carmichael*, 1989). This data is required in different scales of investigation, varying from mineral crystals to planetary bodies and their moons. Increasing the number and variety of available properties, such as density or magnetic properties, produces new inflow data to reduce the ambiguity of geophysical data interpretations. It also broadens the knowledge and spectrum of rock types from sedimentary (carbonates, sandstones) and crystalline rocks (igneous, metamorphic) up to various meteorite impact rocks, and more (*Schön*, 2004).

Most natural rocks are heterogeneous, consisting of components with different physico-chemical properties (Fig. 1.1). For example the magnetic properties, which describe the behavior of matter under influence of magnetic field (*Dunlop and Özdemir*, 1997), divide rocks and minerals to into diamagnetic, paramagnetic and ferromagnetic materials. In diamagnetic materials the electron orbits in the complete electron shells generate the magnetization in the opposite direction from the applied field, yielding slightly negative magnetic susceptibility. In paramagnetic materials electron spins in the incomplete electron shells produce magnetization in the same direction as the applied field, as the unpaired electrons try to partially align the atomic dipole moments to the net magnetization. The resulting susceptibility is small but positive. In ferromagnetic (including ferri-, ferro- and antiferromagnetic) materials the strong interactions between neighboring spins couple spontaneously in a way that aligns the atomic magnetic moments of the same or different magnitude either parallel or antiparallel to one another, resulting in an external net moment and positive magnetic susceptibility. As temperature increases, crystals expand and the exchange interaction becomes weaker. Above a certain temperature, which is characteristic of each crystal type (known as the Curie (T_C) or Neel (T_N) temperature), cooperative spin behavior disappears entirely and the material becomes paramagnetic. This magnetic behavior

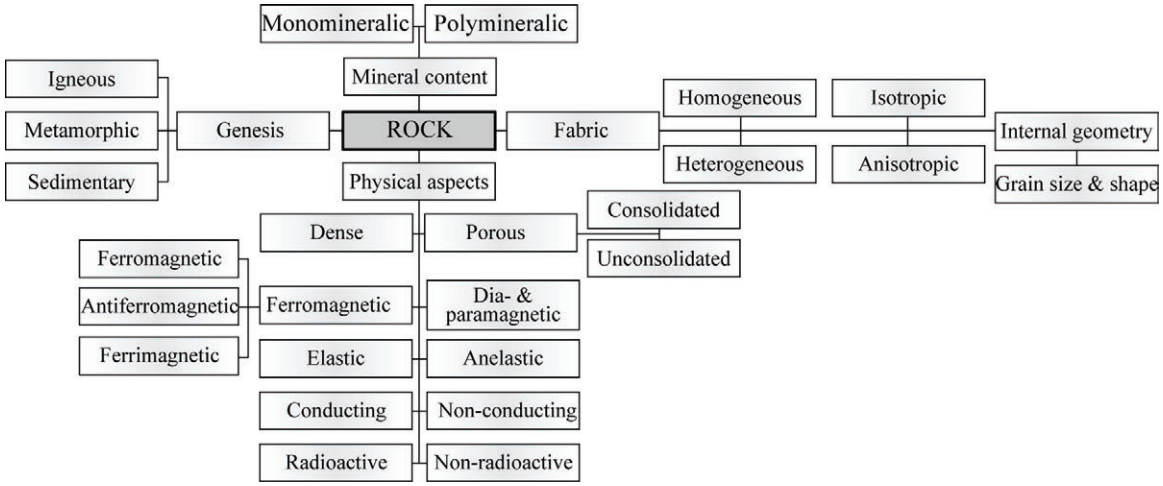

Figure 1.1: A physical property classification scheme of rocks (after *Schön*, 2004)

Table 1.1: Geophysical methods and the corresponding physical properties (after *Schön*, 2004; *Walker and Cohen*, 2007; *Carmichael*, 1989). The methods applied in this thesis are written in italics.

Method	Purpose	Physical property	Outcome of laboratory measurements
Magnetometry e.g. ***Rock-magnetism and Paleomagnetism***	Determination of the magnitude and direction of Earth's magnetic field Mapping of subsurface objects (e.g. ore bodies) Understanding the origin and character of magnetism over time	Magnetic susceptibility Remanent magnetization	Detection of magnetic minerals and magnetized bodies Age dating and reconstruction of movement of the crustal plates
Gravimetry	Mapping of subsurface objects or gravity field Understanding the origin and character of gravity over time	Density	Detection of anomalous density contrasts
Geoelectric and Electromagnetic	Determination of lithology, water level and -saturation, salinity and extent of clay content. Mineral exploration	Electric conductivity Dielectric permittivity Polarization	Electrical properties of the crustal lithologies and identification of highly conductive or resistive bodies
Seismic	Interpretation of subsurface geologic features (e.g. faults, configuration of subsurface layers, identifying potential gas zones)	Velocity Density Elastic properties Reflectivity	Seismic properties of the crustal lithologies and structures
Geothermal	Determination of heat flow and flow direction of fluids and gas	Temperature Thermal conductivity Heat capacity	Heat productivity
Radiometry	Radioactivity surveying Isotope dating	Content of radioactive elements	Geochronology

is described by the existence of magnetic domains, small magnetization regions holding the magnetic moments even in the absence of an external field.

The physical properties of rocks and minerals depend on several factors, namely: (i) the rock type and mineral composition, (ii) the texture and structure, (iii) porosity, pore filling fluid and saturation state, and (iv) grain size, –shape and –distribution (Fig.1.1). For instance, the density of rocks depends on their mineralogy and porosity and is vital in understanding the subsurface geology and geophysics, such as gravity data (Table 1.1). Porosity can result from various geological, physical and chemical processes and determines the characteristics of the reservoirs and influences most of the other physical properties (e.g. density and elastic properties; *Schön*, 2004; *Mayr et al.*, 2008). The physical properties can also be influenced by pressure and temperature, and may vary considerably due to the degree of homogeneity and anisotropy. Although physical properties depend on various factors they also change over time if the rocks have suffered metamorphism or other events, notably impact processes (e.g. *Pesonen et al.*, 1992). Geophysical effects are proportional to the contrast of the physical properties between different rock types (e.g. shock-affected rocks vs. unshocked target rocks). Thus, understanding the subsurface petrophysical structure is important for understanding the crustal features.

1.1 Meteorite impact structures and impact effects

All the terrestrial planets and satellites of the Solar System are covered with craters. The Earth has a violent impact-related history with abundant evidence for an enhanced impact flux at 3.8 Ga. Furthermore, the Moon is believed to have originated through the collision of the proto-Earth with a Mars-sized object (e.g. *Koeberl and Reimold*, 2004). Thus, impact cratering plays a major role in surface forming and -modifying of planetary bodies. It is recognized as one of the fundamental processes in the geological evolution of the Earth (e.g. *French and Koeberl*, 2010, and references therein). Studies on terrestrial impact craters can give necessary information about planetary evolution and influence the terrestrial environment, including the biosphere (*Schulte et al.*, 2010; *Koeberl and MacLeod*, 2002). Some of the terrestrial impact structures, e.g. Vredefort (age 2.02 Ga, 300 km diameter) and Sudbury (age 1.85 Ga, 250 km diameter), are also considered economically important as they are associated with natural resources and significant mineralizations (*Grieve*, 2006; *French*, 1998; *Pilkington and Grieve*, 1992).

Studies of the Earth and the Solar System have revealed that impact cratering is an ongoing and complex geological process. Several tons of extraterrestrial material continually collides with Earth every day, however, most of it is in dust form or small enough to either burn or decelerate in Earth's atmosphere without reaching the surface (*Sharpton,* 2005). Impact structures form when a large cosmic object (projectile), such as an asteroid or a comet, collides with a target body (Earth's surface) at velocities up to 10 - 70 km/s (*Melosh*, 1989; *French*, 1998). This hypervelocity impact is very rapid process, which transforms vast amounts of kinetic energy into enough heat to melt or vaporize the projectile and the target. It generates intense high pressure shock waves (can be up to several hundred GPa near the contact; *French,* 1998), not met by any terrestrial geological process (*Melosh*, 1989). The travelling shock and rarefaction waves metamorphose and fracture rocks and minerals, creating microcrystalline fractures, such as Planar Deformation Features in quartz (PDFs; 10–30 GPa), as well as shatter cones (≥2–30 GPa). Furthermore, the shock waves can convert target rock minerals into new high-pressure mineral phases, e.g. coesite, stishovite, or diaplectic mineral glasses (>30–50 GPa; *French and Koeberl*, 2010).

The impact cratering process can be divided into three main stages (Fig. 1.2; *Melosh*, 1989; *French*, 1998), namely: (i) penetration- (also termed as contact and compression stage), (ii) excavation and (iii) modification- stage. During *penetration stage* the projectile collides with the target and enormous amount of kinetic energy is released and transformed into high pressures and temperatures. The material affected by the impact is compressed and pushed outward from the point of impact while the shock waves travel away and lose the energy due to reduction of the overall energy density with increasing area. The target rock is deformed and heated (*French*, 1998), and the peak pressures decrease rapidly with distance. The duration of the penetration stage is determined by the behavior of the release wave reflected back to the projectile (*French*, 1998) and is of the order of less than a second depending on projectile size, composition and the velocity of the impact. The *excavation stage* and crater opening are carried out by shock waves through the target lithologies. During this stage the tension stress exceeds the mechanical strength (the elasticity) of rocks and fractures the target rocks. The propagating shock may also demagnetize or magnetize the target lithologies (*Gattacceca*, 2010), and together with heat propagation may change the magnetic mineralogy by creating new magnetic phases (*Rebolledo-Vieyra and Urrutia- Fucugauchi*, 2006) or destroying the existing magnetic fraction. The shock-wave energy is converted to kinetic energy resulting in an outward excavation flow around the center of the developing crater, in

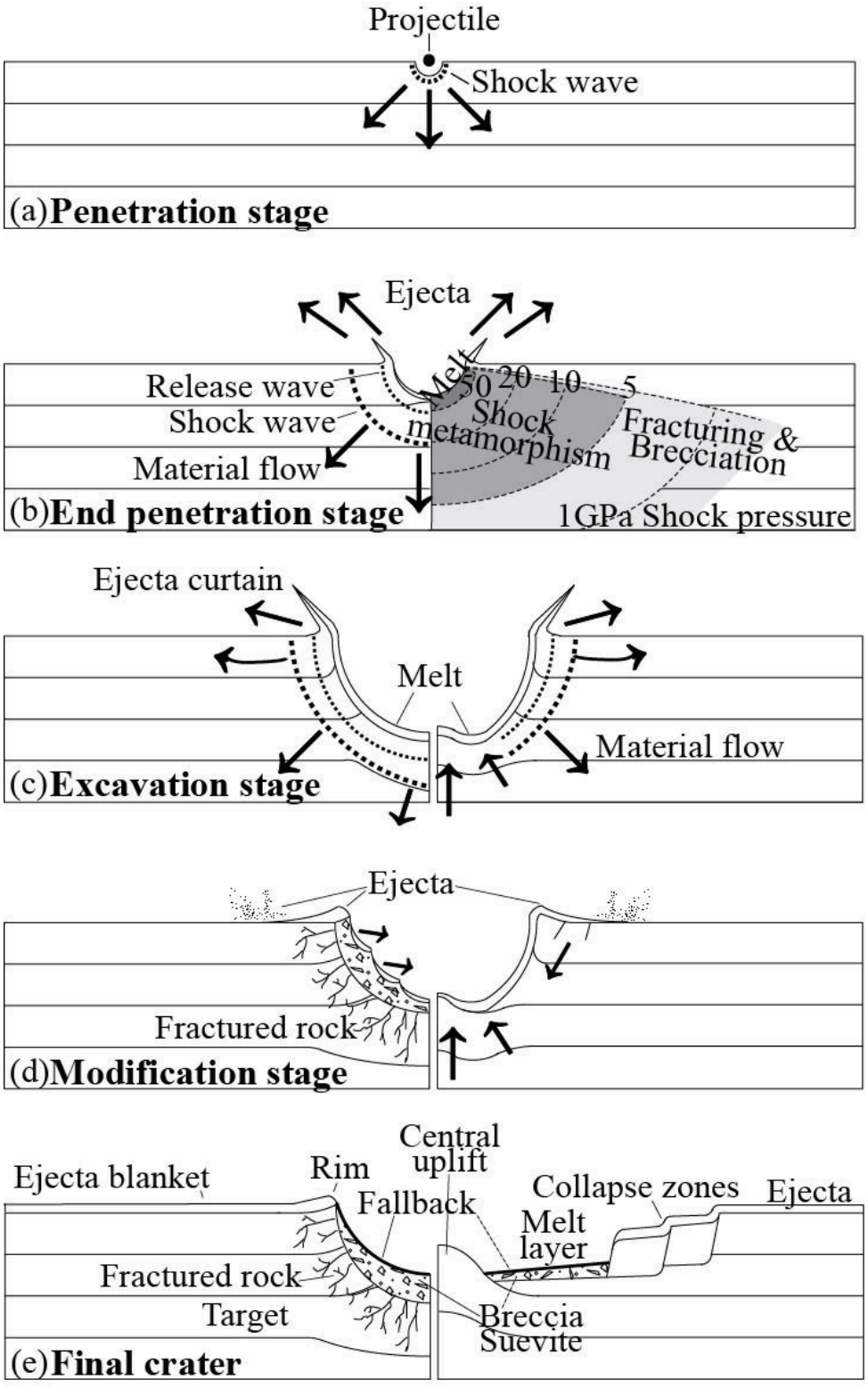

Figure 1.2: Development of an impact structure. (a-b) Penetration or contact-compression stage. The effects of impact at given shock pressures (in GPa) are case specific. (c) Excavation stage; (d) Modification stage; and (e) Final impact structure. The shock wave pressures and the zones of different impact features are presented in (b). The formation of a simple crater, without central uplift, is illustrated on the left side (c-e), and the complex crater, with a central uplift, on the right (c-e). (Modified after *Melosh*, 1989; *French*, 1998).

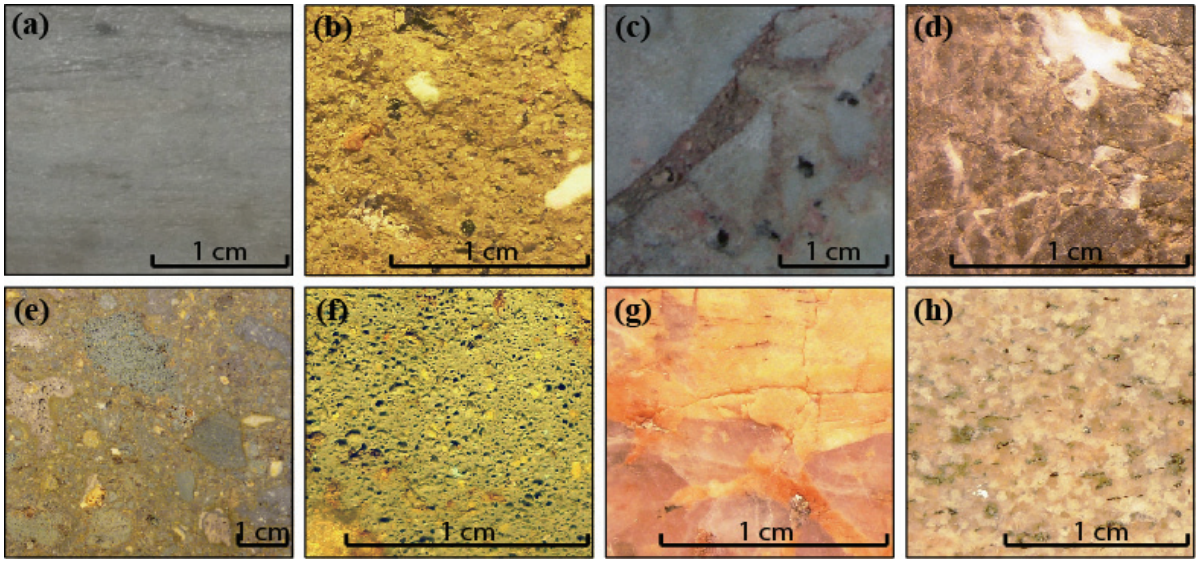

Figure 1.3. Examples of impact, preimpact and postimpact rocks. (a) Postimpact limestone from Yax1 drill core, Chicxulub; (b) sedimentary breccia from Ey1 drill core, Chesapeake Bay; (c) monomict breccia (Yax1); (d) polymict breccia (Ey1); (e) suevite from Bosumtwi; (f) melt (Bosumtwi); (g) fractured target rock (granitoid; Ey1); and (h) un-fractured target rock (granitoid; Ey1).

a transient cavity (*Melosh*, 1989; *French*, 1998) and ejecta curtain, as well as in an uplift of near-surface rocks to form a transient crater ring. During this stage the central peak, in case of the complex crater, also starts to develop. The excavation stage can last from seconds to minutes, depending on the size of the transient crater. During the last, *modification stage* the transient crater grows unstable and its walls start to collapse due to gravity and rock mechanical properties. The collapse partially fills the crater with brecciated, fall-back and melted material (Fig. 1.3). In larger structures slump terraces and central peaks form. The duration of this stage depends on the size of the final structure. During the post-impact processes, due to elevated residual temperatures or hydrothermal activity, the impact- and target rocks may acquire new thermo- or chemoremanent magnetizations (e.g. *Coles and Clark*, 1982) which overprint the previous remanent history, or go through other changes.

Impact craters appear in two morphological forms (*Melosh*, 1989). Small craters (*simple craters*) are simple bowl-shaped depressions with upraised rims (e.g. Barringer crater, Arizona, U.S.A) while larger structures (*complex craters*) are characterized by a central peak (e.g. Bosumtwi, Ghana; Chesapeake Bay, Virginia, U.S.A.) or central peak-ring (Chicxulub, Mexico) and a zone of slumped rock blocks near their outermost rim (Fig. 1.2). The exact transition diameter between these forms depends on target composition (sediment or crystalline) and gravity (*Koeberl and Martinez-Ruiz*, 2003).

At the present, 178 impact structures have been identified on Earth (*Earth Impact Database*, 2010) with a variation of diameters from 0.1 km to 300 km and ages from present to ~2200 Ma. The larger structures include Vredefort in South-Africa (300 km; *Reimold*, 1993; *Gibson and Reimold*, 2001), Sudbury in Canada (250 km; *Deutsch and Grieve*, 1994; *Stöffler et al.*, 1994), and Chicxulub in Mexico (~180 km; *Hildebrand et al.*, 1991). The spatial distribution of impact structures, however, shows that most of these structures are found on continental crust in geologically stable areas and in places with active search strategies and impact structure study programs, such as in Fennoscandia (*Dypvik, et al*., 2008). Recognizing the impact origin of the structures on Earth can be difficult because geological processes such as tectonics, erosion and burial can hamper or remove the evidences of impact cratering (*Pilkington and Grieve*, 1992). Impact structures can be verified by several geological (mainly mineralogical), geophysical and geochemical features. The diagnostic criteria are: (i) morphology, (ii) geophysical anomalies, (iii) evidence of shock metamorphism (e.g. shatter cones or PDFs in quartz grains), and (iv) presence of meteorite fragments or geochemical and isotopic evidence of their traces, e.g. enhancement of the siderophile and platinum group elements (*French and Koeberl*, 2010; *Grieve and Pilkington*, 1996, *Pilkington and Grieve*, 1992, *Koeberl and Anderson* 1996). The circular form of the geological structures can be an indicator for the potential impact structure. The same applies to geophysical features (*Grieve and Pilkington*, 1996), e.g. negative gravity anomaly due to lower density of brecciated rocks in simple craters and positive anomaly due to central uplift and the elevated denser material in complex craters. Similarly, circular magnetic lows associated with small structures (<10 km; e.g. Kärdla, *Plado et al.*, 1996; Bosumtwi; *Plado et al.*, 2000) and high-amplitude anomalies in larger structures (>40 km, *Grieve*, 2006; Ries, *Pohl et al*., 1977) hint to impact origin. Large amounts of information can also be obtained by studying the impact ejecta. In some cases (e.g. Chicxulub and the K/T-boundary) remnants of distal ejecta are found far (> 5000 km) from the impact structure and can give the sole means to discover the buried impact structures and study impact processes. The ejecta, found in normal stratigraphic record can also act as excellent time markers and allow relating the impact event to possible biological effects (*Koeberl and Martinez-Ruiz*, 2003). However, the morphological observations and remote methods can provide only supporting information and not the confirming evidence, while points (iii) and (iv) above are considered definitive criteria. Thus, the possible impact structures must be sampled by field studies. If the structure is not exposed on the surface, deep drilling is required for providing the material.

1.2 Scientific drilling

Past decades have shown an increase in interest for drilling through geologically interesting structures of the uppermost continental crust (*Harms and Emmermann*, 2007). The reason for this is that deep drilling provides an opportunity to study scientifically interesting, yet inaccessible subsurface structures. Drillings reveal direct information on fundamental Earth processes as well as on the evolution of the crust and are used to study the effects of meteorite impacts, mantle plume processes and the nature of tectonic processes. Thus, drilling is an indispensable tool to test the geophysical and geological models derived from surface studies. Furthermore, drilling can also provide information on subjects of societal

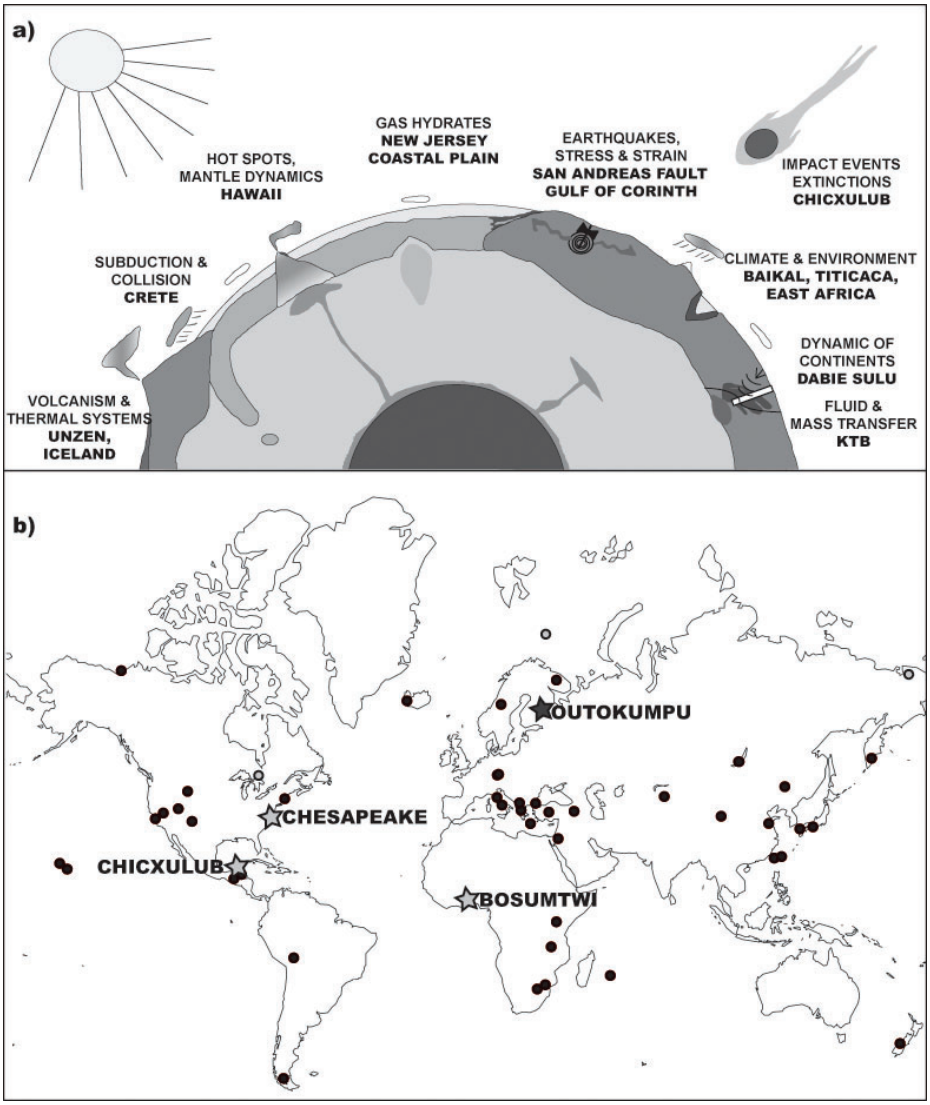

Figure 1.4: (a) The ICDP activities and (b) a schematic distribution map of ICDP project sites (redrawn after *ICDP, 2010*). The location of the drill sites of this study is marked with star – light gray represents impact structures: (i) Bosumtwi, (ii) Chesapeake Bay and (iii) Chicxulub, and black star indicates the location of the Outokumpu drilling site.

relevance, such as the documentation of climate change and the assessment of groundwater resources (*Harms and Emmermann*, 2007).

The drillings of this study were carried out in the framework of the International Continental Scientific Drilling Program (ICDP). The ICDP comprises a cost-effective international research endeavor to explore the composition, structure and globally significant processes of the Earth's crust in localities where drilling is the only option (Fig. 1.4a). The first ICDP drilling project started in 1998 on the Lake Baikal. Since then a total of 21 continental drilling projects with broad international participation have been carried out worldwide (Fig. 1.4b; *ICDP, 2010*) and have led to many important discoveries on paleoclimate, impact cratering, volcanoes, mantle plumes, active faults, etc.

1.3 Aims of the study

Two main objectives were defined for this dissertation. The first objective was to determine the physical properties of the drill core samples in order to contribute to the characterization of different lithologies and to physically delineate the important layers, such as impact layers and ophiolites. In the case of Outokumpu– a continental crust not affected by impact processes – drill cores, the physical properties were also used to explain the distinct crustal reflectors evident in previous seismic reflection studies. For these reasons the basic petrophysical studies, as well as seismic velocity studies in latter case (see Chapter 2: Sampling and methods), were conducted.

The second main objective was to study and acquire insights of the impact generated changes in the target rocks and magnetic minerals from the Bosumtwi, Chesapeake Bay and Chicxulub impact structures. The characteristics of the magnetic fractions of these structures was defined by numerous rock magnetic and paleomagnetic experiments (see Chapter 2: Sampling and methods). These results were then combined with other petrophysical observations in order to better understand the influence of impact on rock physical properties.

When combined with existing mineralogical, geological and geophysical data, the ground-truth petrophysical data provided by this work can be used for further geophysical modelings (magnetic, gravity, seismic) and is therefore significant for understanding crustal evolution of the planet Earth.

2 Sampling and methods

The deep drillings, described in this dissertation, were carried out between 2001 and 2006 as follows: (i) the Chicxulub Scientific Drilling Project during the winter of 2001/2002; (ii) the Lake Bosumtwi Drilling Project in 2004; (iii) the Outokumpu Deep Drilling Project in 2004/2005; and (iv) the Chesapeake Bay Impact Structure Deep Drilling Project in 2005/2006. In November 2005 Tiiu Elbra participated for two weeks in the Chesapeake Bay on-site drilling activities (Fig. 2.1a). After completion of the respective drilling operations, the drill cores were shipped to core repositories located at the (i) Universidad National Autónoma de México (UNAM) at the Institute of Geophysics, Mexico, (ii) the GeoForschungsZentrum, Potsdam, Germany, (iii) the Geological Survey of Finland (GSF), Loppi, Finland, and (iv) the U.S. Geological Survey (USGS) National Center in Reston, Virginia. In the core repositories the scanning and documentation of the cores took place before making the cores available for scientific team members for sampling.

The sampling for studies described in this dissertation was done in several phases. The first set (27 samples) of Chicxulub drill core was provided by the UNAM team in autumn 2003. During the 2004-2005 extra sample sets (total of 410 samples) were received from Dr. M. Rebolledo-Vieyra, prof. T. Kenkmann, prof. J. Smit and prof. A. Deutsch to replenish the sampling density, focusing especially on impactites, K-Pg boundary and the lowermost part of the Chicxulub core. To complement the upper core section, additional sampling (20 samples) was carried out in summer 2005 at UNAM core repository by Tiiu Elbra (Fig. 2.1d). The Bosumtwi and Chesapeake drill cores were sampled at the sampling parties (Bosumtwi: Jan. 2005, sampling interval of 1-5 m, total of ~100 samples and Chesapeake: March 2006, 236 samples; Fig. 2.1c). In both cases the complete drilled sequences were displayed, and the cores were examined and sample intervals marked. The Chesapeake sampling was done in co-operation with prof. Y. Popov from the Moscow State Geological Prospecting University, Russia, as both teams required a uniform but dense sampling rate to allow high-resolution physical property data to be extracted. The cutting and shipping of the samples took place in the core repositories following the sampling parties. The Outokumpu samples were received in several sets during 2005-2009 depending on the sample preparation speed at GSF.

All the ICDP drill core samples were half cores (the other half was kept for the project archives) and featured blue-red marking lines, which indicated up-down orientation of the samples (Fig. 2.1 g). Only in the case of the Outokumpu the full cylinders of two different

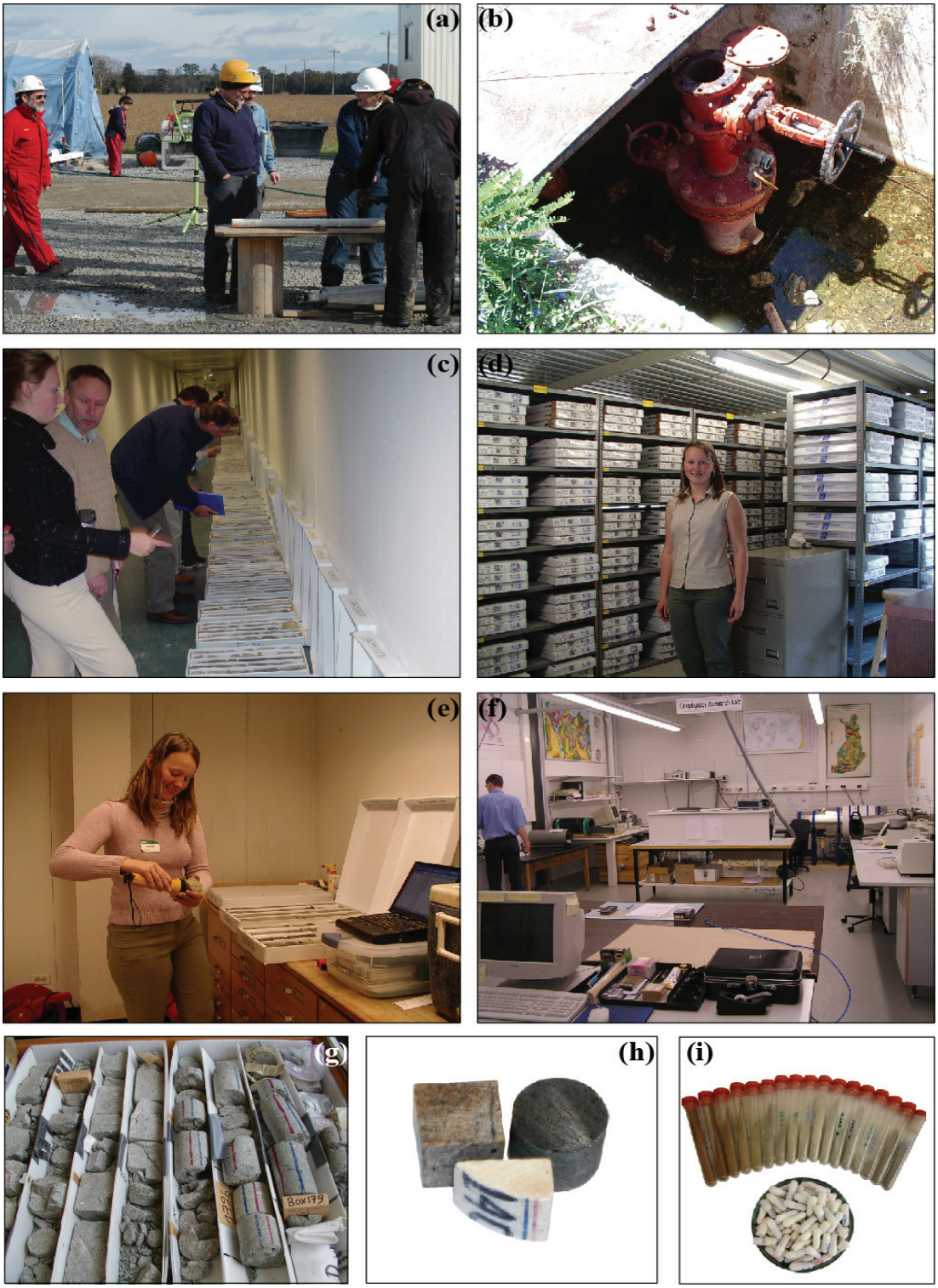

Figure 2.1: From the drilling site to the laboratory. Examples of the drilling sites: during the Chesapeake Bay drilling activity (a), and after the Chicxulub drilling project (b). Sampling: during the Bosumtwi sampling party (c), and additional sampling in UNAM core repository after the Chicxulub sampling party (d). The measurements were carried out in (e) the USGS core storage for the Chesapeake susceptibility logging and in (f) the Solid Earth Geophysics laboratory at the University of Helsinki. (g) Drill core samples with blue-red markings indicating the up-down orientation, (h) various shapes of the specimens for the laboratory petrophysical and paleomagnetic measurements, and (i) powderized specimens for the rock magnetic experiments.

diameters (ø ~ 4 cm, L ~3-7 cm, and ø ~ 2.5 cm, L ~2-2.5 cm) were provided for the investigation.

The samples were prepared in the Solid Earth Geophysics laboratory at the University of Helsinki into 1-3 specimens of three shapes: cylinders, cubes and prism-like shapes, depending on sample fragility and size of the half-cores (Fig. 2.1 h). For rock magnetic measurements powder samples were prepared out of the cores (Fig. 2.1 i).

2.1 Basic petrophysical studies

The basic petrophysical measurements of wet density (ρ; hereafter called density), grain density (ρ_G), porosity (ϕ), magnetic susceptibility (κ), and intensity of Natural Remanent Magnetization (*NRM*) were carried out prior to rock magnetic or seismic velocity studies. For density and porosity measurements the Archimedean method, based on weighing the water saturated and dried samples in the air and in the water, was used. In the case of unconsolidated or extremely fragile samples, the dry density measurements were carried out using tiny glass beads (*Consolmagno and Britt*, 1998) as replacement for water. The magnetic susceptibility was measured using a RISTO-5 kappabridge (operating frequency of 1025 Hz, and field intensity 48 A/m) and AGICO (Advanced Geoscience Instruments Company) KLY-3S kappabridge (operating frequency 875 Hz and field intensity 300 A/m). Furthermore, the magnetic susceptibility of the entire Chesapeake core (over 2300 measurements) was measured at the USGS in March 2006 prior to the sampling party using an AGICO KT-6 field kappameter (operating frequency 10 kHz) to complement to the missing geophysical borehole loggings (*Gohn et al.*, 2009; *Heidinger et al*., 2009). The *NRM* measurements were performed using a 2G Superconducting Rock Magnetometer. The Koenigsberger ratio (Q), a ratio of the remanent magnetization to the induced magnetization, was calculated from measured *NRM* and susceptibility: the used inducing fields at each study latitude were adopted from the National Geophysical Data Center (*NGDC*, 2010) based on coordinates of the drill-hole location. In general when $Q > 1$ the remanent magnetization is stronger than the induced magnetization and the specimen is able to maintain a stable remanence (e.g. *Stacey and Banerjee*, 1974).

2.2 Rock magnetic studies

2.2.1 Temperature dependence of magnetic susceptibility

To gain the knowledge of the magnetic mineralogy, temperature dependence of magnetic susceptibility (*κ-T* curves; Fig. 2.2) was conducted in an argon atmosphere over a temperature range of -192° to 700°C. The Curie (*Tc*) and Neel (T_N) temperatures were obtained by monitoring the susceptibilities in varying temperatures and detecting the temperature, above which the material becomes paramagnetic. As this temperature is specific for each ferromagnetic (incl. antiferro- and ferrimagnetic) mineral, knowing the T_C and T_N allows the distinction between different magnetic minerals (Table 2.1; e.g. *Dunlop and Özdemir*, 1997).

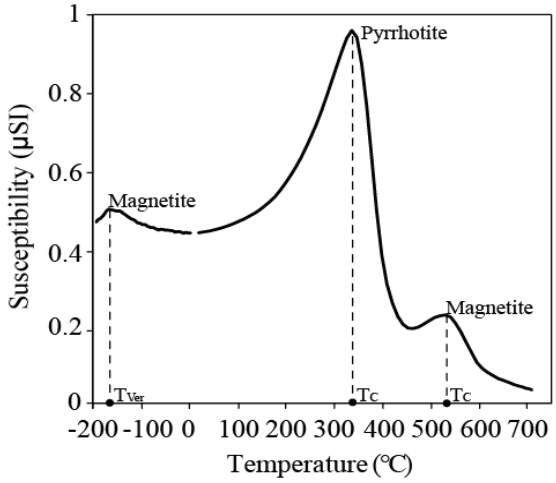

Figure 2.2: Example of low- and high temperature thermomagnetic measurements of the suevite sample from Eyreville drill core (Chesapeake) indicating the Verwey transition (T_{Ver}) and Curie temperatures (*Tc*) for pyrrhotite and magnetite. (Modified after Paper **III**).

The *κ-T* was measured using an AGICO KLY-3S kappabridge in conjunction with a CS-3/CS-L heating furnace. To obtain the low temperatures, liquid nitrogen was used and then flushed off with argon gas before the measurement. During both the low- (-192°- 0°C) and high-temperature (~20°-700°C) runs the magnetic susceptibility was recorded. From these data the T_C or T_N; (Table 2.1), as well as low temperature transitions (Verwey T_{Ver}, Morin T_M), were extracted. Sometimes the irreversible behavior was observed in heating and cooling curves with the formation of new magnetic minerals, as a result of oxidation or reduction (*Dunlop and Özdemir*, 1997).

Table 2.1: Rock magnetic properties of common ferromagnetic minerals (e.g. *Dunlop and Özdemir*, 1997; *Carmichael*, 1989)

Mineral	**Composition**	**κ (SI)**	**$T_{Ver, M, INV}$ (C°)**	**$T_{C, N}$ (C°)**	**M_S (kA/m)**	**H_C (T)**
Magnetite	Fe_3O_4	1.2-19.2	-153	580	480	0.1-0.25
Titanomagnetite	$Fe_{3-x}Ti_xO_4$			150-540	125	0.2
Maghemite	γFe_2O_3		<250	590-675	380	~0.1
Hematite	αFe_2O_3	$0.5\text{-}30*10^{-3}$	-15	675	≈2.5	2.5-7.6
Pyrrhotite	Fe_7S_8	0.001-6	(-240)	320	≈80	0.2-0.35
Goethite	αFeOOH			120	≈2	2.2

T_{Ver} – Verwey transition, T_M – Morin transition, T_{INV} – Inversion temperature, T_C – Curie temperature, T_N – Neel temperature, M_S – Saturation magnetization, H_C – Coercivity

2.2.2 Magnetic hysteresis and First Order Reversal Curves

Only a finite amount of electronic magnetic moments within a given volume attempt to align in the presence of an external field (e.g. *Dunlop and Özdemir*, 1997; *Carmichael*, 1989). When the alignment is complete, the magnetization reaches saturation. The magnetically saturated ferromagnetic material will not relax back to zero magnetization when the external magnetizing field is removed. This "magnetic memory effect", called remanent magnetization, can be removed by applying a field in the opposite direction and is the basis of magnetic hysteresis. Hysteresis is related to the existence of magnetic domains in the material. The atomic magnetic moments of electron spins in the smallest magnetized particles so-called single domain (SD) particles, attempt to remain as parallel (or anti-parallel) as possible to one another. As particle size increases to pseudo-single domain (PSD) size, the external energy is minimized by deviating from strict parallelism to some extent. Eventually, in the multi-domain (MD) particles, the domain walls start to form (e.g. *Dunlop and Özdemir*, 1997; *Carmichael*, 1989). To verify the magnetic fraction and identify the domain states (and thus the magnetic grain size distribution) the measurements of magnetic hysteresis and First Order Reversal Curves (FORCs) were carried out.

The magnetic hysteresis (Fig. 2.3) and FORCs were measured at room temperature using a Princeton Micromag 3900 VSM (Vibrating Sample Magnetometer) instrument with 2 in. laboratory electromagnet (applied field max: 1 T). The FORC data were processed with a code provided by Winklhofer (*Winklhofer and Zimanyi*, 2006). For magnetite, the obtained ratios M_{RS}/M_S and H_{CR}/H_C from hysteresis measurements were plotted in Day-plots (Fig. 2.4; *Day et al.*, 1977) and were used to determine the domain state in specimens.

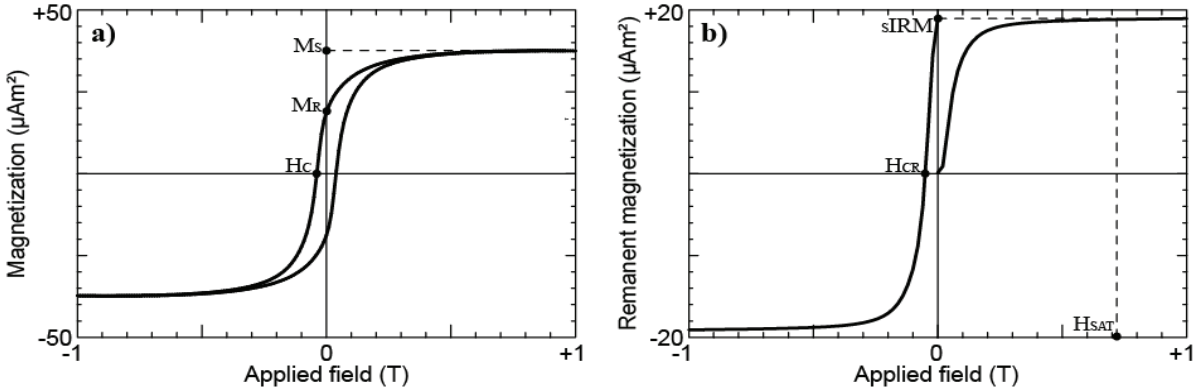

Figure 2.3: Example of (a) magnetic hysteresis and (b) remanence for mixture of pyrrhotite and magnetite in the suevite sample from Eyreville drill core (Chesapeake). The M_S stands for saturation magnetization, M_R stands for saturation remanent magnetization, H_C is coercivity, H_{CR} coercivity of remanence, $_S$IRM saturation isothermal remanent magnetization, and H_{SAT} indicates the necessary field to saturate the magnetization. (Modified after Paper **III**).

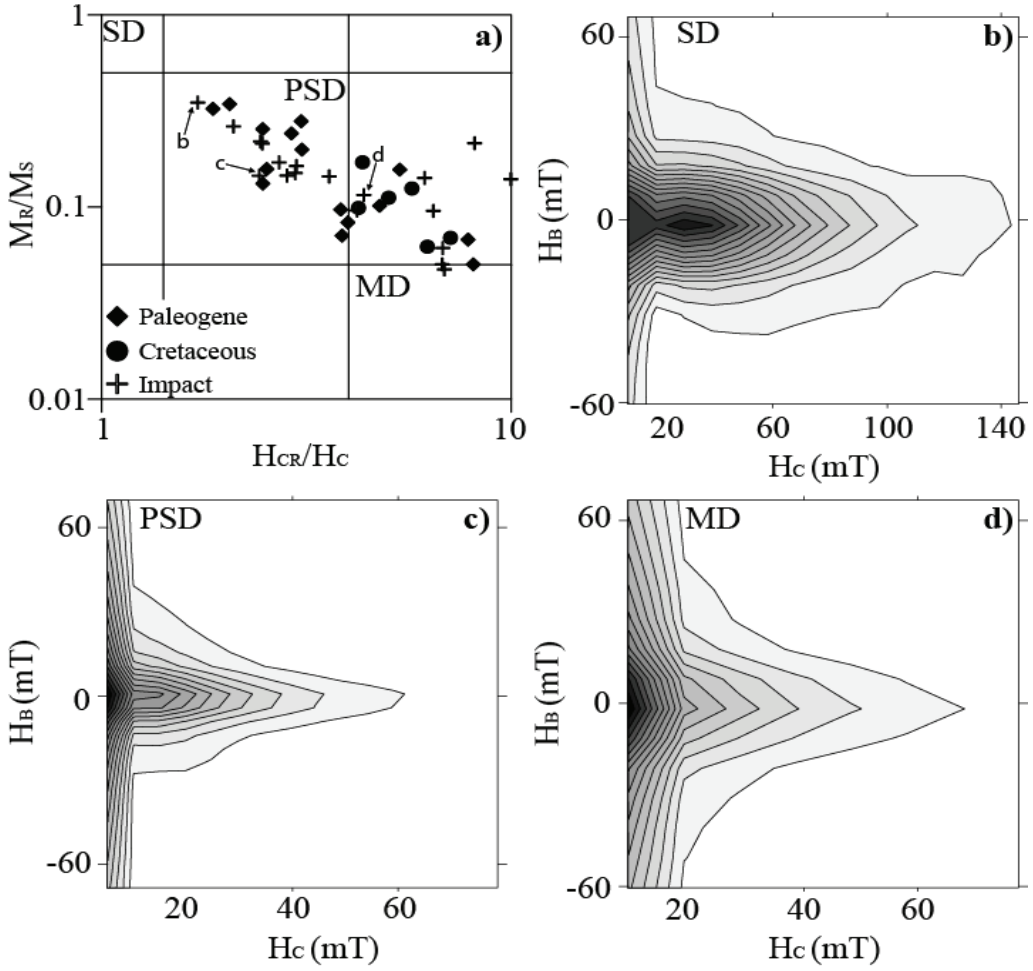

Figure 2.4: Example of (a) Day-plot (*Day et al.*, 1977) and (b-d) FORC diagrams of samples from Yax-1 drill core (Chicxulub), indicating the coercivity distribution and domain size (SD single domain, PSD pseudo-single domain, and MD multi domain).The arrows in the Day plot point to the samples displayed in (b-d). (b, c) Chocolate-brown melt breccias and (d) variegated polymict melt breccia. (Redrawn after Paper **IV**).

2.2.3 Anisotropy of magnetic susceptibility

The magnetic susceptibility of rocks correlates to the magnetic mineral content. Magnetically isotropic rock specimens consist of randomly oriented magnetic grains with no preferred orientation. However, various phenomena such as magma flow, tectonics, shock, etc. (e.g. *Tarling and Hrouda*, 1993) may align the magnetic grains and subsequently the susceptibility takes the maximum value along the preferred alignment of the grains. Thus, the anisotropy of magnetic susceptibility describes the internal structure and the influence of rock forming processes.

The anisotropy of magnetic susceptibility measurements were carried out using the AGICO KLY-3S kappabridge, which allows the automatic measurements of susceptibility along three perpendicular axes while the specimen is rotating. The degree of anisotropy (*P'*), inclination of foliation (*Incl F*) and shape factor (*T*) were derived from these measurements.

2.3 Paleomagnetic studies

Rocks and minerals may retain a variety of forms of remanent magnetizations depending on their magnetic properties, geologic origin and history. The objective of paleomagnetic studies was to separate the remanence components, e.g. the characteristic remanence component (ChRM), and to identify the origin and carriers of these components. The directional information along with intensities and coercivities were extracted using the alternating field demagnetization (*AF*), in some cases also thermal demagnetization (*TH*). Due to merely up-down orientation of the cores, with no azimuthal orientation, only inclination data is used for analysis.

The paleomagnetic measurements were conducted with a 2G DC-SQUID Superconducting Rock Magnetometer. During the *AF* demagnetization a progressively increasing alternating magnetic field was applied to specimens at room temperature using 22 steps (2.5–10 mT steps) until the peak field of 160 mT. In the stepwise *TH* demagnetization the samples were heated to temperatures below and around the Curie temperature of common ferromagnetic minerals (Table 2.1) and afterward cooled back to room temperature in the magnetic vacuum. Following each temperature step the susceptibility, to monitor alterations in magnetic mineralogy, and remaining remanent magnetization were measured. Thermal demagnetizations were performed using the Schoenstedt TDS-1 and Magnetic Measurements

MMTD1 furnaces. Additionally, a few TH measurements were done in Paleomagnetic Laboratory in Pruhonice using the MAVACS (Magnetic Vacuum Control System; *Příhoda, et al.,* 1988-1989) in combination with AGICO JR-6A Spinner Magnetometer.

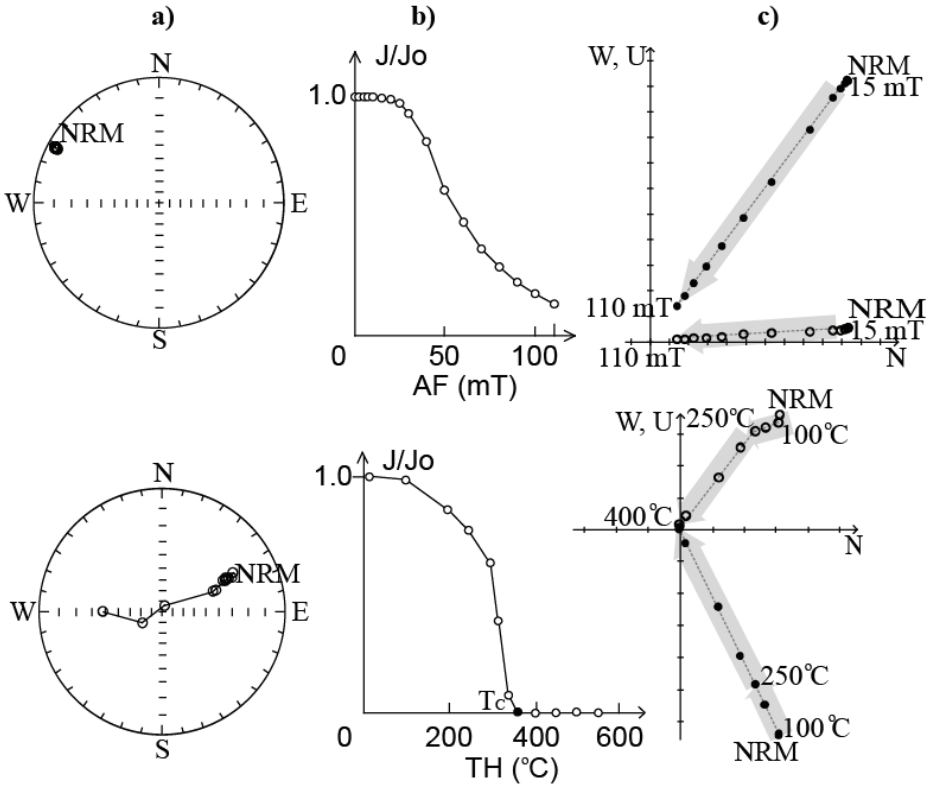

Figure 2.5: Examples of alternating field (AF) and thermal (TH) demagnetization. (a) Stereographic projections, and (b) intensity (J/Jo) decay curves of remanence directions, where J_O represents initial NRM intensity. (c) Orthogonal (Zijderveld) vector projections, with W (west), N (north) and U (up/down) components. The natural remanent magnetization is marked with NRM. Closed (open) circles denote projections of the total magnetization vector tip onto the horizontal or vertical plane, respectively. Remanence components are presented by gray arrows. The displayed breccia from LB-07A drill core (Bosumtwi) shows reversed polarity magnetization that is carried by medium coercive mineral with unblocking temperature ~350°C, represented most possibly by pyrrhotite (modified after Paper **I**).

2.4 Seismic velocity studies

The Earth's crust is a solid but elastic medium, which allows the propagation of traveling (seismic) waves. In a solid material the seismic waves can be either longitudinal (P-wave; V_P) or shear (S-wave; *Vs*) waves. While any material, solid or liquid, is subject to compression, V_P propagates through any material, whereas *Vs* depends upon the resistance to shear force, which does not exist in a liquid medium and, thus, *Vs* propagates only in solid matter (e.g. *Schön,* 2004). The velocity propagation depends on the physical nature of the material, such as density and elasticity, and is, therefore, varying in different rocks. Thus, the seismic

velocities of rocks characterize the nature of the crust and can also be used to find lithological and geophysical interpretations of e.g. the distinct crustal reflectors as observed in seismic surveys (*Kukkonen et al.*, 2006).

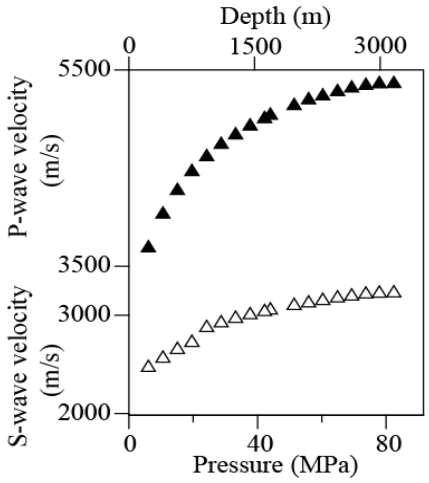

Figure 2.6: V_P and V_S velocities, as a function of pressure and depth, of diopside-tremolite skarn from Outokumpu drill core.

Longitudinal and shear wave velocities of the Outokumpu Deep Drill Core were measured under crustal temperatures and pressures using a novel custom built ultrasonic instrument (*Lassila et al.*, 2010). Velocity measurements (Fig. 2.6) were performed under uniaxial compression. The seismic impedances, Young's modulus, Poisson's ratios as well as the reflection coefficients for various lithological units and their boundaries were obtained from measured velocity data.

Furthermore, the seismic P-wave velocities of more than 1700 water saturated samples were measured (in ≤1 m intervals whenever the core allowed) at ambient pressure with a velocity apparatus developed and situated at the GSF.

3 Summary of the results

3.1 Physical properties of drill cores

Drill cores from three impact structures (Bosumtwi, Chesapeake and Chicxulub) and one non-impact continental crust site (Outokumpu) were used to characterize the physical properties of various lithologies in order to understand the subsurface structures and to provide constrains for geophysical modelings. Results of these studies are presented in Papers **I**, **III**, **IV** and **V**.

Paper **I** focuses on the petrophysical and paleomagnetic investigations of the two ~500 m deep cores, LB-07A and LB-08A (6° 30' N, 1° 25' W), from the Bosumtwi impact structure. The 1.07 Ma old Bosumtwi complex structure (ø 10.5 km) is located in the Ashanti Province in Ghana, West Africa. The Bosumtwi area, segment of the West African Craton, is dominated by Proterozoic Tarkwaian-Birimian (~2.2–1.9 Ga) age target rocks, such as metasediments and metamorphosed volcanites. The crater itself is filled by a lake and covered by postimpact sediments, and is the source crater for the Ivory Coast tektites (*Koeberl et al.,* 1998). Rare outcrops of ejected suevites occur mainly north of the crater. The studied drill cores comprise of both impactites and the target rocks, i.e. meta-greywacke and metapelites.

Results of the petrophysical studies indicate that impactites and various target lithologies can be distinguished by their physical properties. The measured porosities of impactites were extremely high (up to 38%) and the densities significantly lower than in target metasediments. As the grain densities remained constant throughout impactites and target lithologies, the lower bulk densities were interpreted to be related to the formation mechanism of the impactite units, including brecciation and fracturing. On average, the porosity of lithic breccias was higher in LB-07A (27%) than in LB-08A (15%) due to stronger brecciation and lower consolidation state in the former case. The magnetic susceptibility of the cores showed mostly a paramagnetic signature with only minor inhomogeneously strewn ferromagnetic components. Although the NRM varied throughout the examined interval, slightly lower values were found in the upper part of the LB-08A drill core due to differences in magneto-mineralogy.

The complex behavior of physical properties of rocks, resulting from lithological variations, coupled with impact induced variations is described in Papers **III** and **IV**. Paper **III** presents the data of the Eyreville core (Ey-1) from the Chesapeake Bay impact structure. Chesapeake is a 35 Ma-old complex impact structure that is located in Virginia, U.S.A., near the mouth of Chesapeake Bay. The diameter of Chesapeake structure is ~85 km, which indicates the margins of the outer rim. It is one of the four submarine/subaerial impact structures still covered by oceanic waters (*Poag et al.*, 2003). The drilling site (37° 19' 18" N, 75° 58' 32" W) was located on a private land at the Eyreville Farm, in the Northampton County, about 7 km north of the town of Cape Charles, and consist of three holes (Ey-1 A-C; *Gohn et al*., 2009) with a total depth of 1766 m. The cores penetrate through a complete section of the

post-impact Eocene to Pliocene marine and Pleistocene paralic sediments, and through the impacted rocks. The latter include Exmore sedimentary breccias and Cretaceous sediment blocks, suevitic and lithic impact breccias, a granitic megablock, and basement-derived rocks, such as schists and pegmatites with minor gneiss and a few impact-generated breccia veins.

The physical properties reveal a large inhomogeneity along the Ey-1 core but allowed the distinction between different sections. The post-impact sediments showed the lowest density (<1800 kg m^{-3}) and highest porosity (up to 65%) with gradually increasing density and decreasing porosity throughout the Exmore section toward the Cretaceous sediment blocks (Fig. 2 in Paper **III**). The density and porosity (≤1%) of the granitoids is homogeneous, whereas the schist-pegmatite section as well as impact breccias showed large scale variations. The sedimentary deposits, including the postimpact sediments and the diamictons of the Exmore beds, are characterized by weak magnetizations. The rhythmic variation of different lithologies was identified causing the intrinsic pattern of magnetic susceptibility. The ferromagnetic signal was seen in impact breccias (~300-6000 μSI), which showed wide range variations depending on the mineral composition. The granitoids above the breccias were magnetically distinctly more susceptible than the rest of the core.

Paper **IV** describes physical properties of the Yaxcopoil (Yax-1) drill core in the Chicxulub impact structure. Chicxulub structure is situated in the Yucatan carbonate platform, half on- and half off-shore, in the northern part of the Yucatan peninsula, southeastern Mexico. Chicxulub is one of the largest (ø 180 km) multi-ring impact structures on Earth. It was formed 65 Ma ago into sedimentary units overlying the crystalline basement by a vast hypervelocity impact resulting in one of the three largest mass extinctions and marking the transition from the Mesozoic to the Cenozoic at the K-Pg boundary. The drilling was carried out in Hacienda Yaxcopoil (20° 44' 38.45" N, 89° 43' 06.70" W), 62 km from the crater center, in the southern sector of the Chicxulub structure. A borehole penetrated through postimpact Tertiary sediments and impact sequence into preimpact Cretaceous megablocks in its deepest (1511 m) end.

Different physical properties characterize the various lithologies, such as impactite units and the K-Pg boundary layer. In general, the impactites displayed averagely lower density (2266 kg m^{-3}) with wide range of porosities (0.5-33.9%). The postimpact sediments indicated large scale variations within the full depth range of the section. Despite the variations in density and porosity, the grain density was found relatively uniform throughout the Tertiary

sediments with a slight increase with depth towards impact units. The preimpact lithologies consist of denser material with several higher density (>2900 kg m^{-3}) zones. Unlike postimpact rocks, the preimpact lithologies showed high variability also in grain densities. This indicates that physical properties of preimpact lithologies were mainly dominated by mineralogical composition rather than porosity as was observed in case of postimpact and impact rocks. The magnetic properties showed dia- or paramagnetic behavior for 90% of the core. This excludes the impactite section, which was separated by higher susceptibility and remanence values. The contrast of the impactites to the target and to postimpact lithologies was sharp, reflecting the impact formation mechanism, and allowed to establish the contact (especially the K-Pg boundary) between.

Paper **V** describes the petrophysical results of the Outokumpu (OKU) drill core, as a part of continental crust which has not suffered any impact event. The Outokumpu region is located in the Fennoscandian Shield, in eastern Finland, close to the Archean- Proterozoic boundary zone. It is known for its occurrences of early Paleoproterozoic sulphide ore deposits associated with an ophiolitic complex that consists of serpentinites, calc-silicate rocks, siliceous rocks and metamorphosed black shales. The rocks of the Outokumpu ophiolitic complex are embedded in mica schists and gneisses. The OKU drill site (62° 43' 04" N, 29° 3' 43" E) is located 2 km SE from the Outokumpu town. The borehole is 2516 m deep and runs through metasediments, e.g. mica schists from the upper and lower schist series, and ophiolitic rocks into pegmatite-granite complex (Fig. 1b in Paper **V**).

Different lithological units were identified based on their physical properties. With exception of ophiolitic rocks, the density and porosity of the samples remained nearly constant throughout the drilled section. Although only minor porosity (<1%) was observed, it had strong influence on seismic velocities (for further list of parameters influencing seismic velocities see Chapter 3.3: Seismic and elastic properties of upper crust), which exhibited large variations. The velocity in the upper schist series was distinctly lower than of the ophiolitic complex. The pegmatites at the bottom of the core exhibited slightly higher velocities than the samples from the lower schist series but lower than the values of the rocks from the upper schist series. Weak depth dependence in seismic P-wave velocity, density and porosity was also observed. The overall magnetic susceptibilities and remanence distribution helped to distinguish between the magnetically weak schist series rocks and occasionally ferromagnetic rocks in the ophiolite series.

Table 3.1: Petrophysical properties of various lithologies. (after **I**, **III**, **IV**, and **V**).

Lithology	**ρ**	**ρ_G**	**ϕ**	**κ**	**NRM**
Postimpact	2156	2506	23.5	77	0.96
Yax-1	*2328*	*2641*	*18.0*	*46*	*1.15*
Ey-1	*1878*	*2397*	*31.3*	*127*	*0.89*
Impact					
Suevite	2314	2561	13.9	813	71.66
Yax-1	*2347*	*2653*	*9.0*	*554*	*22.28*
Ey-1	*2315*	*2542*	*14.7*	*1507*	*116.90*
LB07, LB08	*2242*	*2580*	*21.9*	*516*	*59.39*
Breccia	2281	2668	19.8	1907	162.14
Yax-1	*2269*	*2696*	*18.3*	*2587*	*192.94*
Ey-1	*2198*	*2509*	*20.6*	*380*	*10.26*
LB07, LB08	*2317*	*2661*	*21.6*	*420*	*86.39*
Preimpact (*non-impact)	2681	2739	3.6	1457	191.50
Yax-1	*2633*	*2779*	*10.3*	*17*	*0.17*
Ey-1	*2641*	*2674*	*1.2*	*10327*	*1925.24*
LB07, LB08	*2609*	*2735*	*8.8*	*450*	*36.11*
**OKU*	*2734*	*2738*	*0.6*	*731*	*3.96*

ρ - density (kg m^{-3}), ρ_G – grain density (kg m^{-3}), ϕ - porosity (%), κ - magnetic susceptibility (μSI), NRM – natural remanent magnetization (mA m^{-1})

The petrophysical results of the meteorite impact cases as well as the Outokumpu case (as part of a normal, non-impact, crust), were combined and are shown in Table 3.1 and Fig. 3.1. The drill core samples from the three impact structures denote that densities of the preimpact target rocks are mostly high, with average density of >2600 kg m^{-3} for all sites (Table 3.1; Papers **I**, **III**, **IV**). These data are in accordance with values reported for carbonate and crystalline rocks of non-impact crustal areas (e.g. *Preeden, et al.*, 2008; and Paper **V**). Porosity of the target lithologies is two-folded: the sedimentary target rocks exhibit moderate porosity (~10%) whereas the crystalline basement displays only minor porosity (~1%). The site means of grain densities differ considerably within the drilled sections indicating that the physical properties of preimpact rocks are mainly controlled by their mineral composition (e.g. *Mayr et al.*, 2008) rather than porosity.

The impact lithologies are characterized by higher porosity and lower density than those of target rocks (Table 3.1; Papers **I**, **III**, **IV**). The average densities of impact breccias and suevites are between 2200 and 2347 kg m^{-3}, and the porosities between 9 and 22%. The

average grain density of the breccias and suevites is also lower than those for the target rocks. In Bosumtwi the grain densities display nearly identical values for the breccia and meta-greywacke units (Paper **I**), while being lower than that of metapelites. This indicates that breccias and meta-greywackes hold similar mineralogical composition. Similarly, the impactites from Chicxulub show high contribution of the target rocks (Paper **IV**). Nevertheless, the physical properties of impact breccias and suevites are dominated by differences in porosity rather than mineralogy (Papers **I**, **III**, **IV**; see also Chapter 3.2: The effects of impact onto physical and rock-magnetic properties). The postimpact sedimentary sequences display a wide range of the densities and porosities with uniform grain density distribution, construing the diversity in sedimentation and diagenesis.

The magnetization of the examined postimpact rocks and sediments is generally low (Table 3.1; Papers **I**, **III**, **IV**). The magnetic susceptibilities range from –200 to 500 μSI and intensities of NRM are between 0.02 and 9 mA m^{-1} (Papers **I**, **III**, **IV**). The most conspicuous difference within the unshocked lithologies is that the (meta-) sedimentary units are mainly dia- or paramagnetic (Papers **I**, **IV** and **V**) while crystalline target (Paper **III**) is occasionally highly magnetic (Table 3.1; Figs. 3.1 and 3.2). In general, the impact lithologies indicated higher magnetic susceptibilities and NRM than the sedimentary target rocks but lower magnetization than crystalline basement (Papers **I**, **III**, **IV**).

The correlation between different physical properties (Fig.3.1) shows that the lithologies can be distinguished from each other by means of density, porosity and magnetic susceptibility. The magnetic susceptibility vs. density and vs. porosity divides the samples into four domains. (i) The majority of the samples from impact lithologies have susceptibility > 200 μSI and density <2610 kg m^{-3} (Papers **I**, **III**, **IV**). The porosity of the impactites is on average >5%. The suevites and breccias indicate overlapping physical properties and hence could not be clearly differentiated from one another. (ii) The crystalline rocks reveal varying magnetization values but high density, with only minor porosity (Papers **III** and **V**), whereas (iii) the sedimentary rocks indicate mostly dia- or paramagnetic behavior while having moderate to high densities >2400 kg m^{-3} and porosity >15% (Papers **I**, **IV**). However, it must be noted that latter two allocated domains may overlap as magnetic susceptibility depends generally on mineralogy rather than on lithology. (iv) The sediment units show both low susceptibilities, with dia- or paramagnetic signal, and low densities, while porosities vary considerably depending on lithification stage of the samples. While magnetic susceptibility

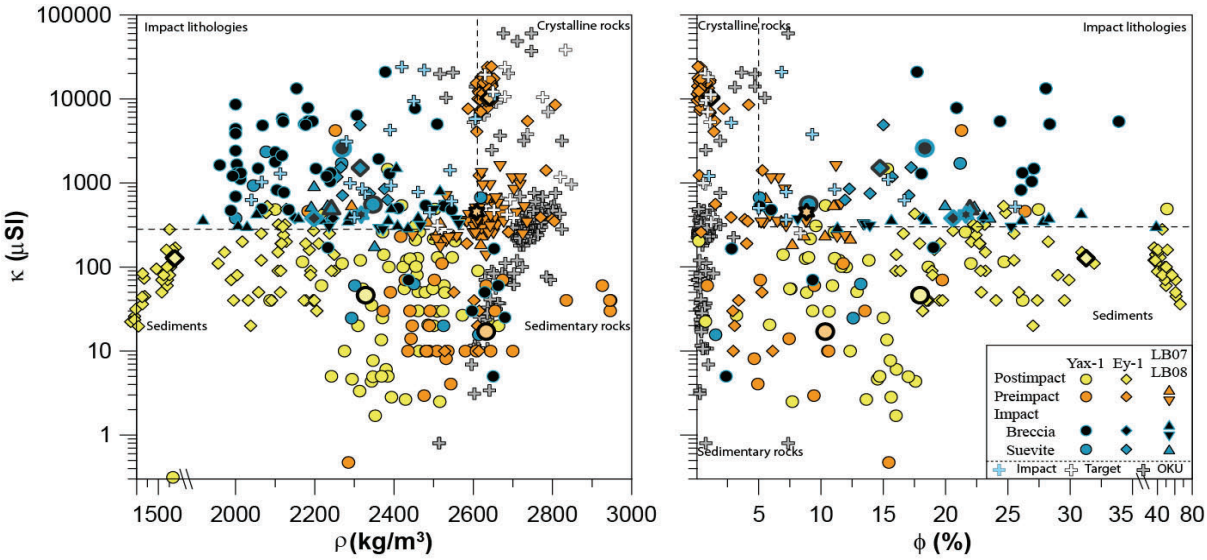

Figure 3.1: Petrophysical properties as a function of lithology (after Papers **I, III, IV**). Dashed lines allocate the area of impactites. Crosses represent impact breccias and unshocked target lithologies from literature (after *Donadini et al.*, 2006; *Henkel*, 1992; *Kukkonen et al.*, 1992; *Pesonen et al.*, 1992, 1999, 2004; *Pilkington et al.*, 2002; *Plado et al.*, 1996, 2000; *Popov et al.*, 2003; *Raiskila et al.*, submitted*; Salminen et al.*, 2006, 2009; *Ugalde et al.*, 2005; *Werner et al.*, 2002) together with Outokumpu samples as a non-impact reference (Paper **V**).

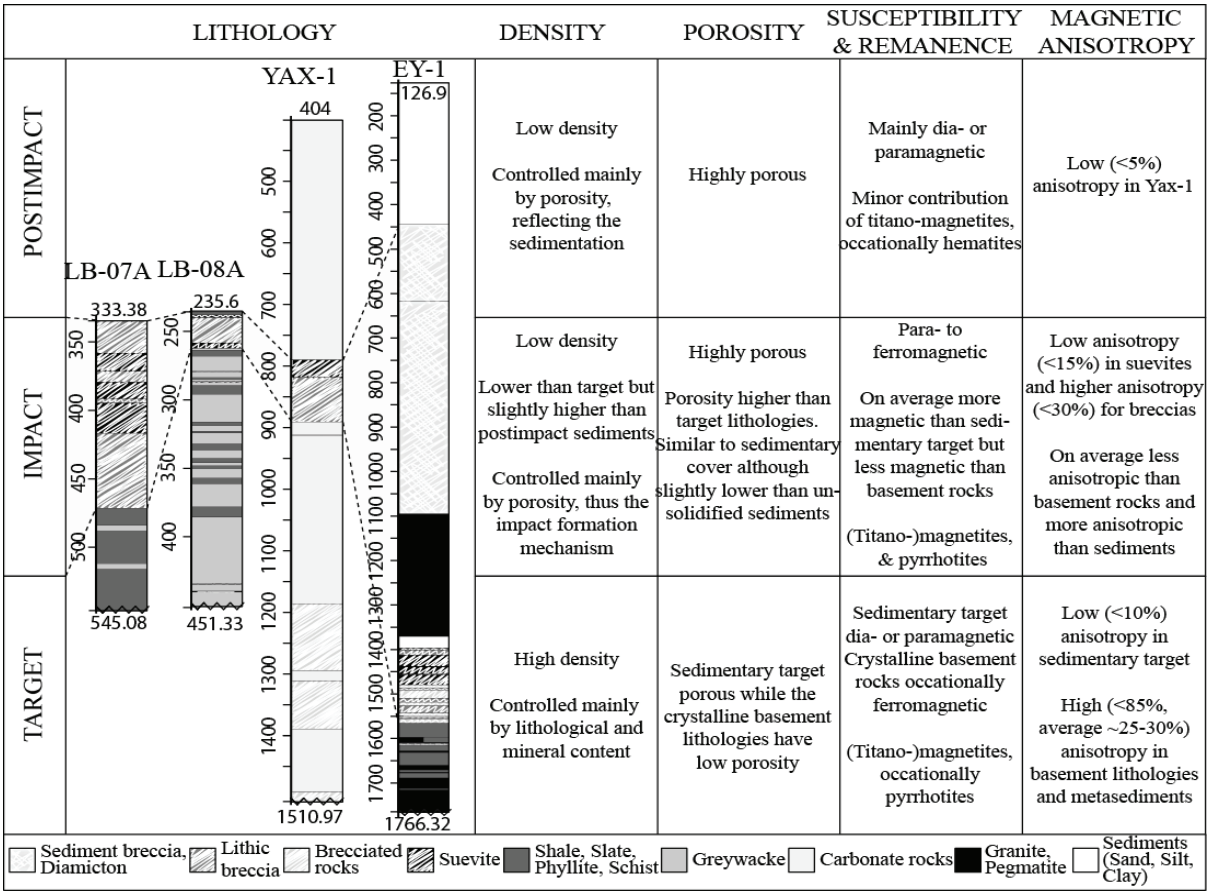

Figure 3.2: Physical characteristics of pre-, postimpact and impact lithologies (after Papers **I, III, IV**).

correlates positively with NRM for all the units the distinct areas of the lithologies are not recognized.

The petrophysical data of Outokumpu (as part of non-impact basement; Paper **V**) as well as data reported for variety of impact structures, such as Jänisjärvi, Karikkoselkä, Keurusselkä, Lappajärvi, Suvasvesi North, Suvasvesi South, Mien, Dellen, Kärdla, Ilyinets, Bosumtwi, Ries, Kara, Popigai, and Vredefort, are in a good agreement with data obtained by this study and support the allocated domains (Fig. 3.1 and references therein).

This new petrophysical ground-truth data of impactites, as well as of target lithologies (Table 3.1; see also Table 1 in Papers **I**, **IV**, and **V**, and Fig.2 in Paper **III**), is useful and necessary for further geophysical modelings (e.g. *Ugalde et al.*, 2007 who used petrophysical data from Papers **I** and **II** to create new magnetic model to explain the magnetic anomaly in Bosumtwi impact structure) in order to reduce the ambiguity of geophysical data interpretations.

3.2 The effects of impact onto physical and rock magnetic properties

Impact cratering is a complex phenomenon, which influences the environment through a multitude of direct or indirect processes. The impact events generate a wide range of structural, shock, and thermal effects in the target rocks, which are dependent on the conditions of formation, distribution, and preservation associated with the impact (*French and Koeberl*, 2010). The characteristics of the magnetic fraction and the impact generated changes in the drilled rocks and magnetic minerals are presented in Papers **I-IV**.

Petrophysical and paleomagnetic studies of the Bosumtwi drill cores (Paper **I**) revealed that the observed high porosity and the fragile nature of impactites are due to the strong brecciation down to the micrometer scale as well as the degree of low consolidation. The relation to the impact formation mechanism was also attained from the grain densities, which displayed constant values in the breccia and meta-greywacke units. The paleomagnetic data revealed the presence of a shallow normal polarization characteristic component (ChRM). This component was suggested to represent the Lower Jaramillo N-polarity chron direction. Based on magnetization direction and behavior, as well as on consistency with the surface data (*Plado et al*., 2000), and the ^{87}Rb-^{87}Sr, ^{39}Ar-^{40}Ar and fission-track dating (e.g. *Kolbe et al.*, 1967; *Koeberl et al*., 1997), this component was assumed to be impact shock related

TRM. Our results suggest that magnetic parameters are related to inhomogeneously distributed ferromagnetic pyrrhotite.

The petrophysical studies of Paper **I** were complemented by the detailed rock magnetic and magnetic mineralogy experiments presented in Paper **II**. Analyses were done in order to understand the magnetic behavior of impact and target lithologies and impact-related remagnetization. The data suggest that the drill cores lost their pre-shock remanence during the impact event at heterogeneous shock pressures between 10 and ~30 GPa (*Deutsch et al.*, 2007; *Ferrière et al.*, 2007; *Coney et al.*, 2007) and acquired a new stable remanence during the shock-induced grain fragmentation. The brecciated and fragmented ferromagnetic pyrrhotites show large grain size variations. However, the detected abundant stress-induced nanostructures in pyrrhotites were assumed to behave as single-domain grains and were interpreted to be responsible for the observed stable remanence acquisition in temperatures not higher than 250°C.

The rock magnetic results (Paper **III**) from the basement-derived and the impact-breccia lithologies of the Ey-1 core, Chesapeake impact structure, imply that pyrrhotites and magnetite carry the magnetic properties. Minor amount of hematite is present in oxidized clays from the uppermost Exmore units and related sediment megablocks. Low abundance of titano-magnetites occurs in diamictons, resulting in mainly paramagnetic behavior for the sediments. The granitic megablock section is magnetically distinctly more susceptible due to the large concentration of magnetite, which also carries the remanence.

The petrophysical results, e.g. homogeneity of density and porosity, and the lack of brittle deformation in magnetite, implied the unshocked nature of the granitoids, which have detached and slid during the collapse of the transient-crater rim (*Horton et al.*, 2007; *Koeberl et al.*, 2007; *Kenkmann et al.*, 2009). The occurrence of alteration zones in the lower part of the block suggested that the displacement surfaces were activated along “weak” zones in the granites. Although the magnetic fabric reveal that granites appear as a single unit, the megablock can be divided into two, upper (oblate shape) and lower (prolate), parts. The boundary between these parts resides close to the transition of the Neoproterozoic gneissic granites and finer-grained Permian-Triassic granites lacking a pronounced fabric orientation in the lower part. The paleomagnetic studies appeared to be consistent with a 250 Ma shallow inclination of North America revealing the preimpact Permian-Triassic remagnetization for the Neoproterozoic granites. This confirmed that the impact did not affect the characteristic

remanence of the granitoids and correlates well with the undeformed nature of the granitic megablock.

In contrast, the impactite sequence below the megablock shows brittle deformation and magnetic fabric randomization, and the pyrrhotite in the associated schist fragments was fractured. The Fe-oxides in granite clasts from the upper part of impactite sequence showed strong desorption features and a porous texture, which indicate melting. The decrease in magnetic susceptibility toward the bottom of the impactite sequence and the subsequent decrease in the melt fragment proportion were observed. The magnetic minerals, pyrrhotite and magnetite, were found significantly oxidized within the impact-breccia unit, indicating a strong degree of alteration. The paleomagnetic results revealed the presence of stable steep-to-medium inclined normal polarity remanence. The stable remanence is typical for impact structures (e.g. Papers **I-II**).

The schist-pegmatite section (Fig. 2 in Paper **III**) revealed a strong heterogeneity with a gradual downward trend of the physical properties and suggested a decrease in shock level (observed also by *Horton et al.*, 2009) and shock-induced fracturing. The high anisotropy, but distinctly lower susceptibility than in megablock granitoids, is believed to reflect the abundance of magnetite in the granitoid varieties. The SD pyrrhotite in the schists was strongly fractured (see also Paper **II**).

Paper **IV** reports the results of the Yaxcopoil drill core, Chicxulub impact structure. The physical properties of preimpact megablock sequence showed no significant traces of impact-induced deformation and brecciation as reported by *Kenkmann et al.* (2004). Dependence on lithology rather than fabric was observed and interpreted either as (i) confirmation of the unity of the megablock, showing the transport of the block during terrace faulting rather than represent ejected material (e.g. *Mayr et al.*, 2008) or as (ii) a result of the decrease in impact induced effects due to recompression of the brecciated megablocks (e.g. Grieve 1988; Plado 1996). It must also be noted that due to scaling differences the shock effects might not have been traced, as the laboratory samples are too small to see macro-fracturing but are too large to detect micro-scale differences. Despite the low magnetic susceptibility of the preimpact section, the occasional minor ferromagnetic component was seen. The anisotropy, shape factor and the orientation of the magnetic fraction illustrated the fabric randomization and showed the influence of impact and brecciation on target lithologies.

Contrary to lithology dependant preimpact rocks, the impactites reflected the impact formation mechanism. The shape and orientation of the magnetic fraction fluctuated and revealed the inhomogeneous fabric development or influence of impact. The traces of extensive secondary clay mineralization due to the impact melt alteration, and the cementation from percolating fluids have been reported for U3-U6 by e.g., *Mayr et al.*, (2008) and contribute to variations in physical properties. Our studies of the impact units indicated the production of hydrothermal low-temperature magnetites and pyrrhotites, which contributed to enhanced magnetizations in impact lithologies as well as to magnetic anomalies. These results were consistent also with data by e.g., *Rebolledo-Vieyra et al*., (2004). The paleomagnetic data suggested that the impact occurred during the reverse polarity geomagnetic chron 29R, which is in agreement with the isotopic dates of the Chicxulub impact as well as with expected K-Pg boundary polarity (see also *Rebolledo-Vieyra et al*., 2004).

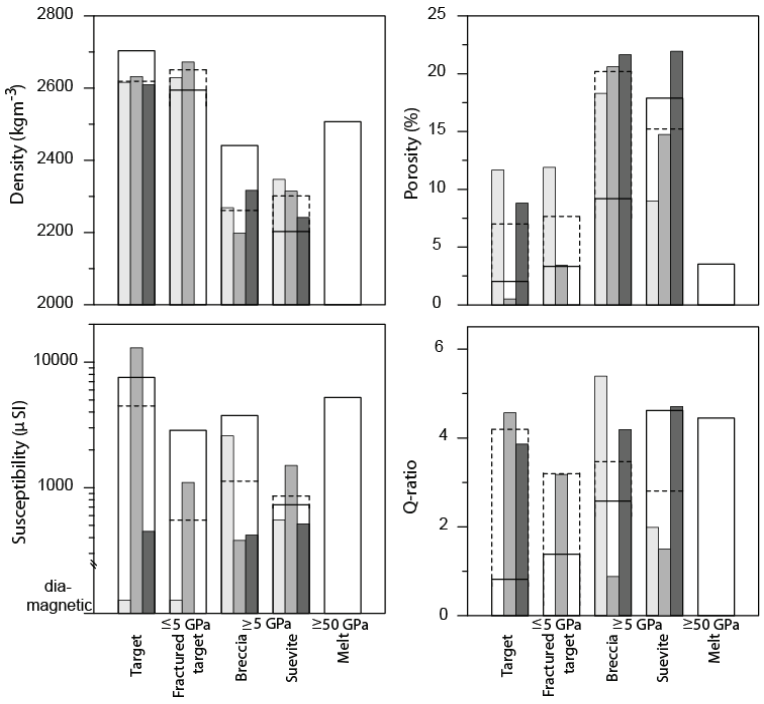

Figure 3.3: Physical properties as a function of lithology and shock pressure. Narrow bars show average values of drill core samples from Chicxulub (light gray), Chesapeake (medium gray), and Bosumtwi (dark gray) impact structures (after Papers **I, III, IV**). Dashed lines show the total average of abovementioned 3 impact structures, while wide white bars indicate the calculated average of 15 impact structures (after *Donadini et al.*, 2006; *Henkel*, 1992; *Kukkonen et al.*, 1992; *Ormö et al.*, 1999; *Pesonen et al.*, 1992, 1999, 2004; *Pilkington et al.*, 2002; *Plado et al.*, 1996, 2000; *Popov et al.*, 2003; *Raiskila et al.*, submitted*; Salminen et al.*, 2006, 2009; *Ugalde et al.*, 2005; *Werner et al.*, 2002). Shock pressures after *French* (1998; look also Fig. 1.2b).

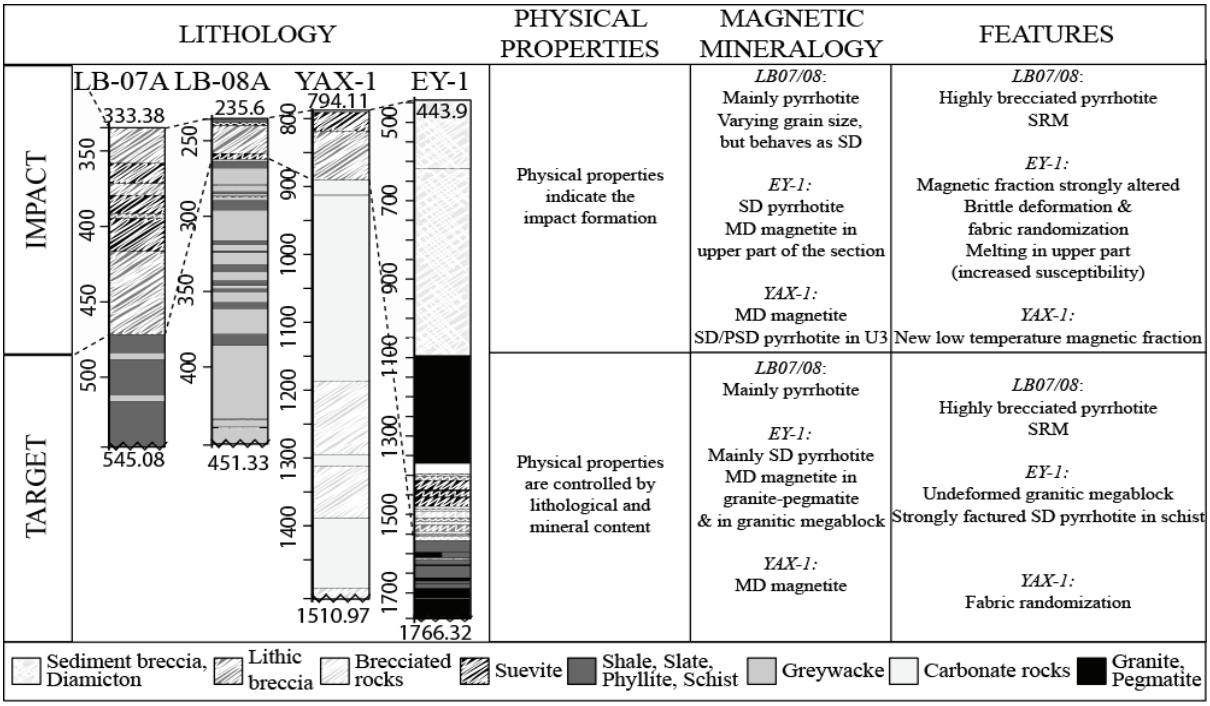

Figure 3.4: Impact effects in preimpact and impact lithologies (Papers **I-IV**).

Several impact effects and features resulting from the shock, melting, crater modification and postimpact hydrothermal systems were distinguished (Figs. 3.3 and 3.4). Petrophysical data (Papers **I-IV**; *Donadini et al.*, 2006; *Henkel*, 1992; *Kukkonen et al.*, 1992; *Ormö et al.*, 1999; *Pesonen et al.*, 1992, 1999, 2004; *Pilkington et al.*, 2002; *Plado et al.*, 1996, 2000; *Popov et al.*, 2003; *Raiskila et al.*, submitted*; Salminen et al.*, 2006, 2009; *Ugalde et al.*, 2005; *Werner et al.*, 2002) indicate a clear decrease in density and increase in porosity from target towards brecciated lithologies due to increasing shock pressure (Fig. 3.3; see also Fig. 1.2b). Slightly higher apparent average density of fractured target than that of unfractured target in this study is due to differences in lithology (e.g. Ey-1: un-fractured granites vs. fractured schists. The latter formed the majority of measured fractured target rocks, thus contribute most to calculated averages. The fractured granitoids at the bottom of the core indicate, however, slightly lower density than that of un-fractured granites, as expected). The magnetic properties did not show such a straightforward trend (Fig.3.3). In the Chicxulub drill core (Paper **IV**; dia- and paramagnetic sedimentary target) the impact increased the magnetic susceptibility. In Chesapeake (Paper **III**; ferromagnetic crystalline target) susceptibility decreased with increasing pressure, whereas in Bosumtwi (Papers **I** and **II**; paramagnetic meta-sedimentary target rocks) susceptibility remained the same. These changes were related to differences in magnetic mineralogy and its distribution. Similarly, either a decrease or an increase in remanent magnetization and Q-ratio have been reported (Fig. 3.3 and references therein). It

should be noted that an increasing trend in Q-ratio in Fig. 3.3 for literature data, is an artifact caused by averaging. Although general trends of shock induced changes in physical properties are seen with increasing shock pressures (Fig. 3.3), the exact pressure limits of these changes are case specific and depend on the lithology, fabric, mechanical stability, magnetic mineralogy and its distribution of the target (e.g., *Grieve et al.*, 1996). To exclude the effect of lithology, a few shock experiments have been conducted to examine the shock effects on the physical properties of rocks on samples of constant lithology or magnetic mineralogy (e.g. petrophysics – *Pesonen et al.*, 1997 and references therein; remanent magnetization – *Gattacceca, et al.,* 2007, 2010, *Louzada et al.,* 2010). As in this study, these studies reveal an increase in porosity (due to fracturing) and a subsequent decrease in density, and either an increase or decrease of magnetic properties. Moreover, the melts do not follow the general trend in physical properties with increasing pressures (Fig. 3.3). The drill cores in this study were scarce in large enough melt fragments to conduct complete petrophysical investigation. However, the lower average density and magnetic susceptibility of melt rocks compared to target lithologies, and higher values than in brecciated and fractured rocks, have been observed in numerous studies (Fig. 3.3 and references therein).

The resulting effects of impact on the physical properties are, thus, multitude and are summarized here based on their occurrence throughout the cratering stages. During the first two stages (penetration and excavation) the rocks are fractured and brecciated, as a result of wave propagation, changing the petrophysical properties: decreasing density and increasing porosity (Fig. 3.3; Paper **I-IV**). Two trends have been reported to occur during shock wave propagation, namely: shock demagnetization, resulting in reduction of NRM, and shock (re-)magnetization (SRM; e.g. *Gattacceca et al.*, 2007, 2010). The demagnetization of remanence during the shock event and shock related remagnetization, as a result of grain size reduction, was observed in this study (Papers **I-II**). *Gattacceca et al.* (2007) also described the shock effects on different lithologies and deducted that intrinsic magnetic properties of shocked rocks suggest, in accordance with the findings of Paper **II**, that the increase in coercivity is attributed to fracturing and/or dislocations of the ferromagnetic grains. In addition to the shock generated changes, impact generated heat produces melt (*French*, 1998), which further changes the composition, including the production, destruction and modification, of the magnetic fraction and its state, and thus changes the properties of rocks. The melting and consequential alteration of the magnetic fraction was observed in Paper **III** and resulted in an increase in susceptibility (see suevites in Fig. 3.3). During the modification

stage, formation of new impact lithologies (impactites) with changed physical properties occur and are clearly distinguishable by density, porosity and magnetic susceptibility (as described above). The re-modification of the fractured bedrock, due to the state of recompression during the raise of the central uplift, may reduce the impact induced effects by decrease in porosity and a subsequent increase in density, as described by *Grieve*, (1988) and *Plado et al.*, (1996; also Paper **IV**). The post-impact processes, such as hydrothermal alteration and oxidation, may further change and modify the magnetic properties by altering the magnetic phases and producing new magnetic minerals (Paper **IV**), and acquire new remanent magnetizations for rocks. Further processes, such as erosion, may remove all impact lithologies so that the remaining structure can be characterized by physical properties of only very weakly shocked target rocks (e.g. Keurusselkä: *Raiskila et al.*, submitted). Fig. 3.3 demonstrates that fractured target rocks have different physical properties than those of unfractured rocks. Thus, the density and porosity measurements are very valuable in this context.

3.3 Seismic and elastic properties of upper crust

The seismic characterization and the elastic properties for OKU drilled section (non-impact crustal formation) are presented in Paper **V**. The results show varying velocities throughout the drill core. The ophiolitic complex (Fig. 1b in Paper **V**), the most distinct section of the core, was identified by its velocity and density highs and lows, thus also by its reflection coefficients. The upper and lower schist series, mineralogically the most uniform rock units (*Kukkonen et al.*, 2007), reveal no distinct differences in any of the petrophysical properties except in the seismic velocity data, which indicated large variations both in the laboratory - and *in situ*–like pressure conditions. The average velocities for various lithologies, e.g. mica schists and diopside-tremolite skarns (V_P 5501 and 6395 m s^{-1}, V_S 3124 and 3645 m s^{-1}, respectively, for *in-situ* pressure conditions; Table 2 in Paper **V**), were obtained. The measured velocities provided the estimates of the seismic impedances, Young's modulus, Poisson's ratios and reflection coefficients for the lithological units of the Outokumpu section.

Previously, a few attempts were made to explain reflections visible in the FIRE-3 reflection data within the 1325.4–1514.3 m interval. *Kukkonen et al.*, (2006) attributed the detected reflectors to the assemblage of ophiolite-related rocks into mica schists. *Heinonen et al.*, (2009; wave sonic log data) and *Kern et al.*, (2009; modeled and measured in pressures up to

600 MPa) reduced the variety of these ophiolites, producing observed reflectors, to serpentinite and diopside-tremolite-skarn with contact into mica schists. The reflection coefficients obtained in this study (*in situ*-like pressure conditions) revealed that the strong and distinct reflections are indeed caused by diopside-tremolite skarns, serpentinites and mica schists as well as black schists. However, the data of this study showed that the reflection contacts are between serpentinites, black schist and mica schist into diopside-tremolite skarn.

The results of seismic velocities revealed also the high significance of the microfracturing, which have dramatically lowered the V_P and V_S values. The variations due to fracturing were reduced when applying upper crustal pressures. Similar observations as well as further effects of pressure, temperature and the sample conditions on velocities of Outokumpu rocks have been reported by e.g. *Kern et al.*, (2009; see also *Elbra et al.*, 2011, *in print*). These studies have revealed a strong velocity dependence on the (i) applied pressure conditions (increase of velocity due to closure of the microcracks); (ii) sample conditions (reflecting the fact that the velocity in water is higher than that in the air filling the pore space in the samples), and (iii) fabric and structural anisotropy related velocity increase and reduction due to preferred orientation (*Kern et al.*, 2009).

Although seismic velocities of impact formations were not addressed in this study, the numerous seismic studies of impact and target lithologies (e.g. *Mayr, et al.*, 2008, 2009; *Schmitt et al.*, 2007; *Vermeesch and Morgan*, 2004; and references therein) have shown similar influence of porosity and its saturation state, microfracturing, and mineral content on velocities as seen in non-impact cases (Outokumpu, in this study). Furthermore, the impact studies have demonstrated that impact induced microcracking and subsequent characteristic lowering of seismic velocities of impactites, compared to those of the undisturbed rocks, depends on the degree of the impact. The decrease of impact damage and an increase in seismic velocities, as well as densities, with depth is indicative of the diminishing shock deformation away from the point of impact. These observations of seismic velocity decrease in the shock affected rocks, in conjunction with knowledge of seismic velocities in typical crustal rocks may be useful for identifying deeply eroded impact structures, which are commonly seen in the Precambrian Shield.

4 Conclusions

The *first* objective of this study was to characterize the different lithologies in meteorite impact structures and in typical Precambrian crustal rocks, and to delineate the various lithological layers according to their physical properties. The physical properties clearly indicated the occurrence of the impact units in Yax-1 drill core (Chicxulub) and LB07A and LB08A drill cores (Bosumtwi), whereas in Ey-1 drill core (Chesapeake) the preimpact granites featured the strongest magnetizations, as well as most homogeneous densities and porosities, while impact lithologies showed large heterogeneity in all physical properties. In the normal, non-impact, crust of the Outokumpu drill core, the ophiolitic section displayed the most distinct signature (including variable density, porosity and susceptibility) compared to the rest of the drilled sections which indicated smaller changes in physical properties.

Based on the petrophysical data the lithologies were divided into four domains: impact lithologies, sediments, sedimentary rocks and crystalline rock. The correlation between different physical properties showed that the lithologies can be distinguished from each other by density, porosity and magnetic susceptibility.

The drill core samples from the three impact structures show that the petrophysics of crystalline target was mostly controlled by its mineral composition, whereas the sedimentary rocks were controlled by either mineral composition or porosity. The physical properties of impact breccias, suevites and postimpact sediments were, however, clearly dominated by differences in porosity, reflecting the formation mechanism of the impactites and in the case of postimpact sediments the diversity in sedimentation sequences.

In the Outokumpu drill cores the physical properties were used to explain the distinct crustal reflectors evident in seismic reflection (FIRE) surveys. The reflection coefficients confirmed that the strong and distinct reflections visible in the FIRE reflection data within the Ophiolitic complex at 1325.4–1514.3 m interval are caused by contacts of diopside-tremolite skarn with serpentinites, black schist or mica schist layers. The results support the data by e.g. *Kern et al.*, (2009) showing the significance of micro-fracturing, which has dramatically reduced the V_P and V_S values. The decrease in seismic velocities due to fracturing was reduced when applying upper crustal pressures in the laboratory.

These large sets of petrophysical ground-truth data obtained for impactites as well as for unshocked lithologies are useful for further geophysical modelings and can help to reduce the ambiguity of geophysical interpretations.

The *second* main objective was to study and acquire insights into the impact generated changes in the target rocks and magnetic minerals, in order to better understand the influence of impact on physical properties. Results of these studies show that the shock damaged the rocks and considerably increased the porosity. The densities of impactites were subsequently reduced relative to those of unshocked target lithologies. In Chesapeake and Bosumtwi (LB-08A) drill cores a slight downward increase in density and decrease in porosity was observed in impact derived units. This suggests a gradual downward decrease of shock-induced fracturing. In the Chicxulub case, a possible re-compression and, thus, reduction of the impact induced effects on porosity and density was seen in the "fractured" bedrock. Additionally, the impactites of all three impact structures covered in this study, indicated a large heterogeneity in physical properties.

The magnetic properties of impact affected rocks showed either an increase or a decrease, depending on the specific case. The differences in magnetizations were related to variations in the magnetic fraction. The shock generated brecciation and fracturing of pyrrhotite in Bosumtwi significantly reduced magnetic grain size, causing pyrrhotites to behave as single-domain grains. Furthermore, the shock demagnetized the existing magnetic fraction and a new remanence was acquired at Lower Jaramillo N-polarity chron during the shock-induced grain size reduction. Similar deformation features in pyrrhotite were also seen in the impact derived rocks of the Chesapeake drill core. Moreover, the melting and consequential alteration of the magnetic minerals was also observed in Chesapeake and resulted in an increase in susceptibility. The impactites from Chicxulub are affected by postimpact low-temperature hydrothermal alteration, which formed new magnetic minerals and subsequently increased the susceptibility and remanent magnetization. The shape and orientation of these magnetic grains was varied and, in addition to hydrothermal activity, reflected influence of the redeposition of impact lithologies. The Chicxulub impact studies also support the idea that impact occurred in reverse polarity geomagnetic chron 29R, which is linked to the K-Pg boundary.

References

Carmichael, R.S. (ed.), 1989. *Practical Handbook of Physical Properties of Rocks and Minerals*. CRC press, Boston, 741 pp.

Gohn, G.S., Koeberl, C., Miller, K.G., and Reimold, W.U., 2009. Deep drilling in the Chesapeake Bay impact structure—An overview. *In:* Gohn, G.S., Koeberl, C., Miller, K.G., and Reimold, W.U., eds., Deep drilling in the Chesapeake Bay impact structure: Geological Society of America Special Papers 2009, **458**, 1-20.

Cockell, C.S., Lee, P., Osinski, G., Horneck, G., and Broady, P., 2002. Impact-induced microbial endolithic habitats. *Meteoritics & Planetary Science*, **37**, 1287-1298.

Coles, R. L., and J. F. Clark, 1982. Lake St. Martin Impact Structure, Manitoba, Canada: Magnetic Anomalies and Magnetizations. *Journal of Geophysical Research*, **87**, 7087 - 7095.

Coney, L., Gibson, R.L., Reimold, W.U., and Koeberl, C., 2007. Lithostratigraphic and petrographic analysis of ICDP drill core LB-07A, Bosumtwi impact structure, Ghana. *Meteoritics & Planetary Science*, **42**, 569–589.

Consolmagno G. J., and Britt D. T. 1998. The density and porosity of meteorites from the Vatican collection. *Meteoritics & Planetary Science*, **33**, 1231–1241.

Day, R., Fuller, M.D., and Schmidt, V.A. 1977. Hysteresis properties of titanomagnetites: Grain size and composition dependence. *Physics of the Earth and Planetary Interiors*, **13**, 260-267.

Deutsch, A., and Grieve, R.A.F., 1994. The Sudbury Structure: constraints on its genesis from Lithoprobe results. *Geophysical Research Letters*, **21**, 963-966.

Deutsch, A., Luetke, S., and Heinrich, V., 2007. The ICDP Lake Bosumtwi impact crater scientific drilling project (Ghana): Core LB-08A litho-log, related ejecta, and shock recovery experiments. *Meteoritics & Planetary Science*, **42**, 635-654.

Donadini, F., Plado, J., Werner, S.C., Salminen, J., Pesonen, L.J., and Lehtinen, M., 2006. New Evidence for Impact from the Suvasvesi South Structure, Central East Finland. *In*: Cockell, C., Koeberl, C., and Gilmour, I., eds., Biological Processes Associated with Impact Events: Springer-Verlag, Berlin, Heidelberg, 287-307.

Dunlop, D.J., and Özdemir, Ö., 1997. *Rock magnetism, Fundamentals and frontiers.* Cambridge University Press, Cambridge, England, 573 pp.

Dypvik, H., Plado, J., Heinberg, C.,Håkansson, E., Pesonen, L.J., Schmitz, B., and Raiskila, S., 2008. Impact structures and events – a Nordic perspective. *Episode*, **31**, 107-113.

Earth Impact Database, 2010. *http://www.unb.ca/passc/ImpactDatabase/index.html*

Elbra, T., Karlqvist, R., Lassila, I., Hæggström, E., Pesonen, L.J., 2011 *in print*. P- and S-wave velocities of rocks from the upper 1.5 km crustal section sampled by the Outokumpu deep drilling, Finland. *Geological Survey of Finland Special Papers*.

French, B.M., and Koeberl, C., 2010. The convincing identification of terrestrial meteorite impact structures: What works, what doesn't, and why. *Earth-Science Reviews*, **98**, 123–170.

French, B.M., 1998. *Traces of a catastrophe: a handbook of shock metamorphic effects in Terrestrial Meteorite Impact Structures.* LPI Contribution, 120, Houston, Lunar and Planetary Institute, 120 pp.

Gattacceca, J., Lamali, A., Rochette, P., Boustie, M., and Berthe, L., 2007. The effects of explosive-driven shocks on the natural remanent magnetization and the magnetic properties of rocks. *Physics of the Earth and Planetary Interiors*, **162**, 85–98, doi: 10.1016/j.pepi.2007.03.006.

Gattaccecaa, J., Boustieb, M., Limac, E., Weissc, B.P., Resseguierb, de T., and Cuq-Lelandaisb, J.P., 2010. Unraveling the simultaneous shock magnetization and demagnetization of rocks. *Physics of the Earth and Planetary Interiors*, **182**, 42–49.

Gibson, R.L., and Reimold, W.U., 2001. The Vredefort Impact Structure, South Africa: The scientific evidence and a two-day excursion guide. *Memoir of the Council for Geoscience*, **92**, 111 pp.

Grieve, R.A.F., 2006. *Impact structures in Canada.* GEOtext 1208–2260, 5, Geological Association of Canada, 210 pp.

Grieve, R.A.F., 1988. The Haughton impact structure: Summary and synthesis of the results of the HISS project. *Meteoritics*, **23**, 249-254.

Grieve, R.A.F., and Pilkington, M., 1996. The signature of terrestrial impact craters. *AGSO Journal of Australian Geology and Geophysics*, **16**, 399-420.

Harms, U., and Emmermann, R., 2007. History and Status of the International Continental Scientific Drilling Program. *In*: Harms, U., Koeberl, C., and Zoback, M.D., eds., Continental Scientific Drilling: A Decade of Progress and Challenge for the Future. Springer, New York, 366 pp.

Heinonen, S., Schijns, H., Schmitt, D.R., Heikkinen, P.J., and Kukkonen, I.T., 2009. High Resolution Reflection Seismic Profiling in Outokumpu. *In*: Kukkonen, I.T. (ed.) Outokumpu Deep Drilling Project, Third International Workshop, 12-13.11.2009, Espoo, Finland. Programme and Abstracts. Geological Survey of Finland, Southern Finland Office, Marine Geology and Geophysics, Report Q10.2/2009/61, 29-31.

Heidinger, P., Wilhelm, H., Popov, Y., Šafanda, J., Burkhardt, H., and Mayr, S., 2009. First results of geothermal investigations, Chesapeake Bay impact structure, Eyreville bore holes. *In*: Gohn, G.S., Koeberl, C., Miller, K.G., and Reimold, W.U., eds., The ICDP-USGS Deep Drilling Project in the Chesapeake Bay Impact Structure: Results from the Eyreville Core Holes: Geological Society of America Special Paper, **458**, doi: 10.1130/2009.2458(39).

Henkel, H., 1992. Geophysical aspects of meteorite impact craters in eroded shield environment, with special emphasis on electric resistivity. *Tectonophysics*, **216**, 63-89.

Hildebrand, A.R., Penfield, G.T., Kring, D.A., Pilkington, M., Camargo, A., Jacobsen, S.B., Boyton, W.B., 1991, Chicxulub Crater: A possible Cretaceous/Tertiary boundary impact crater on the Yucatan Peninsula, Mexico: Geology, 19, 867-871.

Horton, J.W., Jr., Aleinikoff, J.N., Kunk, M.J., Jackson, J.C., Belkin, H., and Chou, I-M., 2007. Initial studies of breccias, blocks, and crystalline rocks in the ICDP-USGS Eyreville-B core, Chesapeake Bay impact structure, 1095–1766 m depth. *Geological Society of America Abstracts with Programs*, **39**, 451.

ICDP, 2010. *http://www.icdp-online.org/*

Kenkmann, T., Collins, G.S., Wittmann, A., Wünnemann, K., Reimold, W.U., and Melosh, H.J., 2009. A model for the formation of the Chesapeake Bay impact crater as revealed by drilling and numerical simulation. In Gohn, G.S., Koeberl, C., Miller, K.G., and Reimold,

W.U., eds., The ICDP-USGS Deep Drilling Project in the Chesapeake Bay Impact Structure: Results from the Eyreville Core Holes, Geological Society of America Special Paper, **458**, doi: 10.1130/2009.2458(25).

Kenkmann, T., Wittmann, A., and Scherler, D., 2004. Structure and impact indicators of the cretaceous sequence of the 1CDP drill core Yaxcopoil-1, Chicxulub impact crater, Mexico. *Meteoritics & Planetary Science*, **39**, 1069-1088.

Kern, H., Mengel, K., Strauss, K., Ivankina, T., Nikitin, A., and Kukkonen, I. 2009. Elastic wave velocities, chemistry and modal mineralogy of crustal rocks sampled by the Outokumpu scientific drill hole: Evidence from lab measurements and modeling. *Physics of the Earth and Planetary Interiors*, **175**, 151-166.

Koeberl C., Bottomley R. J., Glass B. P., and Storzer D. 1997. Geochemistry and age of Ivory Coast tektites and microtektites. *Geochimica et Cosmochimica Acta*, **61**, 1745–1772.

Koeberl, C., Milkereit, B., Overpeck, J.T., Scholz, C.A., Amoako, P.Y.O., Boamah, D., Danuor, S.K., Karp, T., Kueck, J., Hecky, R.E., King, J., and Peck, J.A. 2007. An international and multidisciplinary drilling project into a young complex impact structure: The 2004 ICDP Bosumtwi Impact Crater, Ghana, Drilling Project—An overview. *Meteoritics & Planetary Science*, **42**, 483-511.

Koeberl, C., and Anderson, R. R., eds., 1996. The Mason Impact Structure, Iowa: Anatomy of an Impact Crater. *Geological Society of America Special Paper*, **302**, 468 pp.

Koeberl, C., Reimold, W.U., 2004. Silverpit structure, North Sea:search for Petrographic and geochemical evidence for an impact origin. *Meteoritics & Planetary Science*, **39**, A53.

Koeberl, C., and MacLeod, K.G., Eds., 2002. Catastrophic Events and Mass Extinctions: Impacts and Beyond. *Geological Society of America Special Paper*, **356**, 746 pp.

Koeberl, C., and Martinez-Ruiz, F., Eds., 2003. *Impact Markers in the Stratigraphic Record*. Springer Verlag, New York. 363 pp.

Kolbe, P., Pinson, W. H., Saul, J. M., and Miller, E. W., 1967. Rb-Sr study on country rocks of the Bosumtwi crater, Ghana. *Geochimica et Cosmochimica Acta*, **31**, 869–875.

Kukkonen, I. T., Heikkinen, P., Ekdahl, E., Hjelt, S.-E.,Yliniemi, J., Jalkanen, E. and FIRE Working Group, 2006. Acquisition and geophysical characteristics of reflection seismic data on FIRE transects, Fennoscandian Shield, *Geological Survey of Finland Special Paper*, **43**, 13–43.

Kukkonen, I.T., Kivekäs, L., and Paananen, 1992. Physical properties of kärnäite (impact melt), suevite and impact breccia in the Lappajärvi meteorite crater, Finland. *Tectonophysics*, **216**, 111-122.

Kukkonen, I.T., Kivekäs, L., Safanda, J., and Cermak, V., 2007. Geothermal studies of the Outokumpu deep drill hole, *In*: Kukkonen, I.T., ed., Outokumpu Deep Drilling Project, Second International Workshop, May 21-22, 2007, Espoo, Finland. Programme and Abstracts. Geological Survey of Finland, Southern Finland Office, Marine Geology and Geophysics, Report Q10.2/2007/29, 81-86.

Lassila, I., Karlqvist, R., Elbra, T., Gates, F., Pesonen, L.J., and Hæggström, E. 2010. Ultrasonic velocity of the upper gneiss series rocks from the Outokumpu deep drill hole – comparing uniaxial to triaxial loading. *Journal of Applied Geophysics*, **72**, 178–183.

Louzada, K.L., Stewart, S.T., Weiss, B.P., Gattacceca, J., and Bezaeva, N., 2010. Shock and static pressure demagnetization of pyrrhotite and implications for the Martian crust. *Earth and Planetary Science Letters*, **290**, 90–101.

Mayr, S. I., Wittmann, A., Burkhardt, H., Popov, Y., Romushkevich, R., Bayuk, Heidinger, I.P., and H. Wilhelm, H., 2008. Integrated interpretation of physical properties of rocks of the borehole Yaxcopoil-1 (Chicxulub impact structure). *Journal of Geophysical Research*, **113**, doi:10.1029/2007JB005420.

Melosh, H.J., 1989. *Impact cratering, a geological process*. Oxford monographs on geology and geophysics, **11**, New York, Oxford University Press, 245 pp.

NGDC, 2010. *http://www.ngdc.noaa.gov/geomag/*

Ormö, J., Sturkell, E., Blomqvist, G., and Törnberg, R., 1999. Mutually constrained geophysical data for the evaluation of a proposed impact structure: Lake Hummeln, Sweden. *Tectonophysics*, **311**, 155-177.

Pesonen, L.J., Deutsch, A., Hornemann, U., and Langenhorst, F., 1997. Magnetic properties of diabase samples shocked experimentally in the 4.5 to 35 GPa range. Lunar and Planetary Science XXVIII, March 17-21, Houston, 1087-1088.

Pesonen, L.J., Elo, S., Lehtinen, M., Jokinen, T., Puranen, R., and Kivekäs, L., 1999. Lake Karikkoselkä impact structure, central Finland: New geophysical and Petrographic results. *In*: Dressler, B.O., and Sharpton, V.L., eds., Large Meteorite Impacts and Planetary Evolution II: Boulder, Colorado, Geophysical Society of America Special Paper, **339**, 131-147.

Pesonen, L.J., Mader, D., Gurav, E.P., Koeberl, C., Kinnunen, K.A., Donadini, F., and Handler, R., 2004. Paleomagnetism and $^{40}Ar/^{39}Ar$ Age Determinations of Impactites from the Ilyinets Structure, Ukraine. *In*: Dypvik, H., Burchell, M., and Claeys, P., eds., Cratering in Marine Environments and on Ice: Springer-Verlag, Berlin, Heidelberg, New York, 251-280.

Pesonen, L.J., Marcos, N., and Pipping, F., 1992. Palaeomagnetism of the Lappajärvi impact structure, western Finland. *Tectonophysics*, **216**, 123-142.

Pilkington, M., and Grieve, R.A.F., 1992. The Geophysical Signature of Terrestrial Impact Craters. *Reviews of Geophysics*, **30**, 161-181.

Pilkington, M., Pesonen, L.J., Grieve, R.A.F., and Masaitis, V.L., 2002. Geophysics and Petrophysics of the Popigai Impact Structure, Siberia. *In*: Plado, J., and Pesonen, L.J., eds., Impacts in Precambrian Shields: Springer-Verlag, Berlin, Heidelberg, New York, 87-107.

Plado, J., Pesonen, L.J., Elo, S., Puura, V., and Suuroja, K., 1996. Geophysical research on the Kärdla impact structure, Hiiumaa Island, Estonia. *Meteoritics & Planetary Science*, **31**, 289-298.

Plado, J., Pesonen, L. J., and Puura, V., 1999. Effect of erosion on gravity and magnetic signatures of complex impact structures: Geophysical modeling and applications. *In*: Dressler, B. O. a. S., V.L., ed., Large Meteorite Impacts and Planetary Evolution II: Boulder, Colorado, Geological Society of America Special Paper, **339**, 229-240.

Plado, J., Pesonen, L.J., Koeberl, C., and Elo, S., 2000, The Bosumtwi Meteorite Impact Structure, Ghana: A Magnetic Model. *Meteoritics & Planetary Science*, **35**, 723-732.

Poag, W., Koeberl, C., and Reimold, W.U., eds., 2003. *The Chesapeake Bay Crater: Geology and Geophysics of a Late Eocene Submarine Impact Structure* (Impact Studies), Springer-Verlag, 522 pp.

Pohl, J., Stöffler, D., Gall, H., and Ernston, K., 1977, The Ries Impact Crater. *In*: Roddy, D. J., Pepin, R.O. and Merrill, R.B., ed., Impact and Explosion Cratering, Pergamon Press, p. 343-404.

Popov, Yu., Pohl, J., Romushkevich, R., Tertychnyi, V., and Soffel, H., 2003. Geothermal characteristics of the Ries impact structure. *Geophysical Journal International*, **154**, 355-378.

Preeden, U., Plado, J., Mertanen, S., and Puura V., 2008. Multiply remagnetized Silurian carbonate sequence in Estonia. *Estonian Journal of Earth Sciences*, **57**, 3, 170–180.

Příhoda, K., Krs, M., Pešina B., and Bláha, J., 1988-1989. MAVACS - a new system creating a nonmagnetic environment for palaeomagnetic studies. *In*: E. Banda, ed., Paleomagnetismo - Palaeomagnetism, Cuadernos de Geologia Iberica, CSIC, Madrid, 223-250.

Raiskila, S., Salminen, M.J., Elbra, T., and Pesonen, L.J., *submitted*. Keurusselkä impact structure, central Finland: petrophysical and rock magnetic properties of shocked target rock with paleomagnetic dating. *Meteoritics & Planetary Science*.

Rebolledo-Vieyra, M., and Urrutia Fucugauchi, J., 2004. Magnetostratigraphy of the impact breccias and post-impact carbonates from borehole Yaxcopoil-1, Chicxulub impact crater, Yucatan, Mexico. *Meteoritics & Planetary Science*, **39**, 821-830.

Rebolledo-Vieyra, M., and Urrutia- Fucugauchi, J., 2006. Magnetostratigraphy of the Cretaceous/Tertiary boundary and early Paleocene sedimentary sequence from the Chicxulub Impact Crater. *Earth Planets Space*, **58**, 1309–1314.

Reimold, W.U., 1993. A review of the geology and deformation related to the Vredefort Structure, South Africa. *Journal of Geological Education*, **41**, 106-117.

Robertson, 2010. The interior of the Earth. *http://pubs.usgs.gov/gip/interior/* U.S. Geological Survey. Nov. 18, 2010.

Salminen, J., Donadini, F., Pesonen, L.J., Masaitis, V.K., and Naumov, M., 2006. Paleomagnetism and petrophysics of the Jänisjärvi impact structure, Russian Karelia. *Meteoritics & Planetary Science*, **41**, 1853-1870.

Salminen, J., Pesonen, L.J., Reimold, W.U., Donadini, F., and Gibson, R.L., 2009. Paleomagnetic and rock magnetic study of the Vredefort impact structure and the Johannesburg Dome, Kaapvaal Craton, South Africa – implications for the apparent polar wander path of the Kaapvaal craton during the Mesoproterozoic. *Precambrian Research*, **168**, 167-184.

Schulte, P., Alegret, L., Arenillas, I., Arz, J.A., Barton, B.J., Bown, P.R., Bralower, T.J., Christeson, G.L., Claeys, P., Cockell, C.S., Collins, G.S., Deutsch, A., Goldin, T.J., Goto, K., Grajales-Nishimura, J.M., Grieve, R.A.F., Gulick, S.P.S., Johnson, K.R., Kiessling, W., Koeberl, C., Kring, D.A., MacLeod, K.G., Matsui, T.M., Melosh, J., Montanari, A., Morgan, J.V., Neal, C.R., Nichols, D.J., Norris, R.D., Pierazzo, E., Ravizza, G., Rebolledo-Vieyra, M., Reimold, W.U., Robin, E., Salge, T., Speijer, R.P., Sweet, A.R., Urrutia-Fucugauchi, J., Vajda, V., Whalen, M.T., and Willumsen, Pi.S., 2010. The Chicxulub Asteroid Impact and Mass Extinction at the Cretaceous-Paleogene Boundary. *Science*, **327**, 1214.

Schön J.H. 2004. Physical properties of rocks: Fundamentals and principles of petrophysics. *In*: Helbig, K., and Treitel, S., eds., Handbook of Seismic Exploration, **18**, Elsevier, 583 pp.

Sharpton, V.L., 2005. Meteor. World Book Online Reference Center. World Book, Inc. *http://www.worldbookonline.com/wb/Article?id=ar358140.*

Stacey, F., and Banerjee, S., 1974. *Physical Principles of Rock magnetism*. Elsevier, Amsterdam, 195 pp.

Stoeffler, D., Deutsch, A., Avermann, M., Bischoff, L., Brockmeyer, P., Buhl, D., Lakomy, R., and Mueller-Mohr, V., 1994. The formation of the Sudbury Structure, Canada: towards a unified impact model. *In*: Dressler, B. O., Grieve, R. A. F., and Sharpton, V. L., eds., Large Impact Craters and Planetary Evolution: Boulder, Colorado, Geological Society of America Special Paper, **293**, 303-318.

Tarling, D.H., and Hrouda, F., 1993. *The magnetic anisotropy of rocks*. Chapmann and Hall, London, 217 pp.

Walker, J., and Cohen, H.A., eds., 2007. *The Geoscience Handbook*. Fox River White, 302 pp.

Ugalde, H.A., Artemieva, N., and Milkereit, B., 2005. Magnetization on impact structures – Constraints from numerical modeling and petrophysics. *In*: Kenkmann, T., Hörz, F., and Deutsch, A., eds., Large meteorite impacts III: Boulder, Colorado, Geological Society of America Special Paper, **384**, 25-42.

Werner, S.C., Plado, J., Pesonen, L.J., Janle, P., and Elo, S., 2002. Potential fields and subsurface models of Suvasvesi North impact structure, Finland. *Physics and Chemistry of the Earth*, **27**, 1237-1245.

Winklhofer, M., and Zimanyi, G.T., 2006, Extracting the intrinsic switching fi eld distribution in perpendicular media: A comparative analysis. *Journal of Applied Physics*, **99**, 08E710-1-3.

Appendix 1: Basic parameters, units and equations used in the thesis

Parameter	Symbol	Unit	Equation
Mass	m		
water saturated in air	m_{WA}	g	
water saturated in water	m_{WW}		
dry in air	m_{DA}		
dry in water	m_{DW}		
Volume	V	cm^3	$V = \frac{m_{WA} - m_{WW}}{\rho_W}$
pore volume	V_p		$V_p = \frac{m_{WA} - m_{DA}}{\rho_W}$
Density	ρ	kg/m^3	$\rho = \frac{m}{V}$
density of water	ρ_W		$\rho_{W\ (15\text{-}26°C)} = 999.1 - 996.8$
Porosity	φ	%	$\varphi = \frac{V_p}{V} \times 100$
Magnetic susceptibility	κ	SI	
magnetization	M	A/m	$\kappa = \frac{M}{H}$
magnetic field	H	A/m	
magnetic induction	B	T	$B = \mu_0(H + M)$
magnetic dipole moment	μ	A/m^2	
Remanent magnetization	J or NRM	A/m	
Koenigsberger ratio	Q	-	$Q = \frac{J}{\kappa H}$
Curie, Neel temperature	T_C, T_N	°C	
Verwey transition	T_V		
Morin transition	T_M		
inversion temperature	T_{INV}		
Saturation magnetization	M_S	A/m	
	M_R		
Coercivity	H_C	T	
Coercivity of remanence	H_{CR}	T	
P-wave (longitudinal) velocity	V_P	m/s	
length of sample	L	m	$V_P = \frac{L}{t}$
travel time	t	s	
S-wave (shear) velocity	V_S	m/s	$V_S = \frac{L}{t}$
Poisson's' ratio	ν	-	$\nu = \frac{(\frac{V_P}{V_S})^2 - 2}{2((\frac{V_P}{V_S})^2 - 1)}$
Seismic impedance	Z_P	kg/m^2s	$Z_P = \rho V_P$
Young's modulus	E	GPa	$E = \frac{\mu(3\lambda + 2\mu)}{\mu + \lambda}$
shear modulus	μ		$\mu = \rho V_S^2$
Lame' parameter	λ		$\lambda = \rho V_P^2 - 2\mu$
Seismic reflection coefficient	R_C	-	$R_C = \frac{\rho_2 V_{P2} - \rho_1 V_{P1}}{\rho_2 V_{P2} + \rho_1 V_{P1}}$